Supplementary Information

Enhanced photocatalytic performance of tetraphenylethylene-based porous aromatic frameworks by bandgap adjustment for the synthesis of benzimidazoles

He Wang [a], Xinmeng Xu [a], Linzhu Cao [a], Zhenwei Zhang [b], Jiali Li [b], Xiaoming Liu [b], Xin Tao [a,], Guangshan Zhu [a]*

[a]Key Laboratory of Polyoxometalate and Reticular Material Chemistry of Ministry Education, College of Chemistry, Northeast Normal University, Changchun 130024, P. R. China

[b]College of Chemistry, Jilin University, Changchun 130012, P. R. China

Table of Contents

Materials and characterizations

Materials. Unless otherwise noted, all materials were used as received from commercial sources without further purification.

Instrumentations. The ^{1}H NMR and ^{13}C NMR spectra were obtained in DMSO on Avance NEO 500 spectrometer. ^{13}C CP-MAS solid-state NMR spectra were obtained using a Bruker Avance III model 400 MHz NMR spectrometer at a MAS rate of 5 kHz. Fourier Transform Infrared (FT-IR) analysis was collected in the range of 400 – 4000 cm^{-1}on the Nicolet IS50 Fourier transform infrared spectrometer. The powder X-ray diffraction (PXRD) measurements were carried out on the Rigaku SmartLab X-ray diffractometer with Cu-Kα radiation. The thermogravimetric analysis (TGA) was measured on the METTLER-TOLEDO TGA/DSC 3+ analyzer at the 10 °C min^{-1} in N_2 atmosphere from room temperature to 800 °C. The N_2 adsorption-desorption isotherms were measured at 77 K, using Autosorb iQ2 adsorptometer, Quantachrome Instrument. Samples were degassed at 393 K for 12 h before measurements. The scanning electron microscope (SEM) images were acquired using the JEOL JSM 4800F SEM. Transmission electron microscopic (TEM) images and elemental mapping were acquired by JEOL 2100PLUS instrument at an accelerating voltage of 200 kV. The UV-vis absorption spectra were recorded from 200 – 800 nm on a VARIAN UV-VIS-NIR spectrophotometer (Cary500). The UV-vis diffuse reflectance spectra were recorded using UV-Vis-NIR Spectrophotometer (Cary7000) with $BaSO_4$ used as a reference. The Pd metal loading of obtained polymers was determined by inductively coupled plasma atomic emission spectroscopy (ICP-AES) LEEMAN Prodigy. X-ray photoelectron spectroscopy (XPS) was performed on Thermo Scientific Escalab 250Xi with an Al-Kα X-ray source. The binding energies of elements were calibrated using the C 1s photoelectron peak at 284.8 eV. The electron spin resonance (ESR) was tested by a Bruker EMXplus spectrometer at the X-band frequency (9.4 GHz). 5,5-dimethyl-1-pyrroline N-oxide (DMPO) was used as spin-trapping reagents to detect $O_2^{\bullet-}$. 2,2,6,6-Tetramethyl-4-piperidone hydrochloride (TEMP) was used as spin-trapping reagent to detect $^{1}O_2$. The React IR kinetic experimental spectra were recorded using a React IR 15 with Liquid N_2 MCT Detector, Ag*9.5mm*1.5m Fiber probe Interface and DiComp (Diamond) probe Tip from Mettler-Toledo AutoChem. Data manipulation was carried out using the iC IR software, version 4.3. GC-MS spectra were obtained using

Agilent 5977B GC/MSD. The element analysis was determined by the EA3000 element analyzer. The light irradiation intensity was measured by FZ-A Optical power meter.

Electrochemical measurements. The electrochemical workstation (CHI760E, CH Instruments, Shanghai, China) was used to perform electrochemical measurements on samples. The Glassy carbon electrode, platinum wire electrode and saturated calomel electrode (SCE) are used as working electrode, counter electrode, and reference electrode, respectively. The working electrode was prepared as follows: 0.05 g of sample, 0.10 g of pine alcohol, and 0.005 g of ethyl cellulose were added to an agate mortar and then 5 mL of ethanol was added to it, and the slurry was scraped onto fluorine-doped tin oxide (FTO) glass to form a film for electrical performance testing. The photocurrent measurements were conducted under the irradiation of a 300 W xenon lamp (PLS-SXE300+/UV) in 0.5 M Na_2SO_4, and the test area was 1 cm^2. The electrochemical impedance spectra (EIS) measurements were performed in 0.1 M KCl solution containing 5 mM $[Fe(CN)_6]^{3-/4-}$ at room temperature in the darkness.

Synthesis and Photocatalysis

Synthesis of PAF-364 [1]:

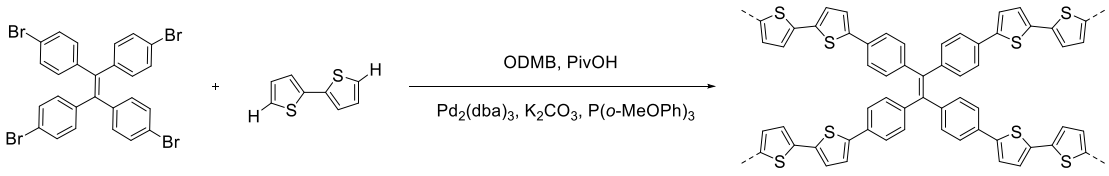

Scheme S1. Synthesis of **PAF-364.**

Under N_2 atmosphere, a mixture of anhydrous 1,2-dimethylbenzene (ODMB) (4 mL), 1,1,2,2-tetrakis(4-bromophenyl)ethene (TPE-4Br) (160.9 mg, 0.25 mmol), 2,2'-bithiophene (BTP) (124.7 mg, 0.75 mmol), anhydrous potassium carbonate (K_2CO_3) (103.5 mg, 0.75 mmol), tris(dibenzylideneacetone)dipalladium ($Pd_2(dba)_3$) (7.00 mg, 0.008 mmol), pivalic acid (PivOH) (15.33 mg, 0.15 mmol) and tris(2-methoxyphenyl)phosphine (P(*o*-MeOPh)$_3$) (5.30 mg, 0.015 mmol) was stirred at 110 °C for 72 h. After the reaction mixture was cooled down to room temperature, the resulting mixture was filtered. The obtained solid was washed sequentially with CH_3OH, H_2O, CH_2Cl_2 and THF, and Soxhlet extracted with CH_2Cl_2 and THF respectively. The obtained solid was then dried in vacuo at 100 °C for 24 h to give an orange-red powder (yield: 82%). The Pd metal loading of PAF-364 was determined by ICP-AES to be 0.2%. Elemental analysis results (%) for PAF-364: C, 72.90; S, 21.24; H, 4.89. The catalytically active unit of PAF-364 is tentatively illustrated as the repeating units: one-fourth of a TPE molecule bonded with half of a BTP (see below).

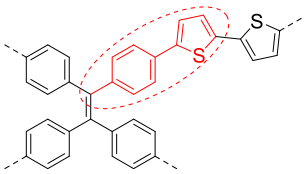

Synthesis of PAF-365 [1]:

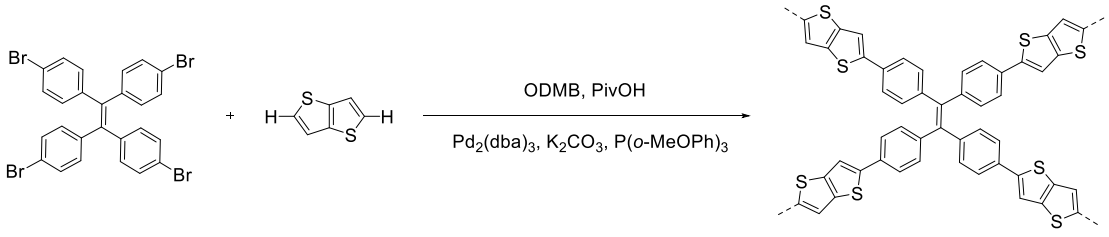

Scheme S2. Synthesis of **PAF-365.**

Under N_2 atmosphere, a mixture of anhydrous ODMB (4 mL), TPE-4Br (160.9 mg, 0.25 mmol), thieno[3,2b]thiophene (TBTP) (105.2 mg, 0.75 mmol), K_2CO_3 (103.5 mg, 0.75 mmol), $Pd_2(dba)_3$ (7.00 mg, 0.008 mmol), PivOH (15.33 mg, 0.15 mmol) and P(*o*-MeOPh)$_3$ (5.30 mg, 0.015 mmol) was stirred at 110 °C for 72 h. After the reaction mixture was cooled down to room temperature, the resulting mixture was filtered. The obtained solid was washed sequentially with CH_3OH, H_2O, CH_2Cl_2 and THF, and Soxhlet extracted with CH_2Cl_2 and THF respectively. The obtained solid was then dried in vacuo at 100 °C for 24 h to give an orange-red powder (yield: 87%). The Pd metal loading of PAF-365 was determined by ICP-AES to be 0.3%. Elemental analysis results (%) for PAF-365: C, 69.65; S, 22.45; H, 3.25. The catalytically active unit of PAF-365 is tentatively illustrated as the repeating units: one-fourth of a TPE molecule bonded with half of a TBTP (see below).

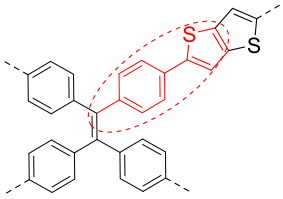

Synthesis of PAF-366 [1]:

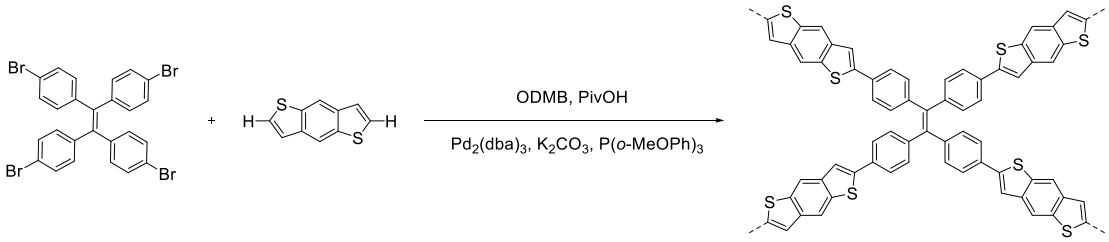

Scheme S3. Synthesis of **PAF-366.**

Under N_2 atmosphere, a mixture of anhydrous ODMB (4 mL), TPE-4Br (160.9 mg, 0.25 mmol), benzo[1,2-b:4,5-b']dithiophene (BDTP) (142.7 mg, 0.75 mmol) K_2CO_3 (103.5 mg, 0.75 mmol), $Pd_2(dba)_3$ (7.00 mg, 0.008 mmol), PivOH (15.33 mg, 0.15 mmol) and P(*o*-MeOPh)$_3$ (5.30 mg, 0.015 mmol) was stirred at 110 °C for 72 h. After the reaction mixture was cooled down to room temperature, the resulting mixture was filtered. The obtained solid was washed sequentially with CH_3OH, H_2O, CH_2Cl_2 and THF, and Soxhlet extracted with CH_2Cl_2 and THF respectively. The obtained solid was then dried in vacuo at 100 °C for 24 h to give yellow powder (yield: 84%). The Pd metal loading of PAF-366 was determined by ICP-AES to be 0.2%. Elemental analysis results (%) for PAF-366: C, 69.33; S, 20.17; H, 3.43. The catalytically active unit of PAF-366 is

tentatively illustrated as the repeating units: one-fourth of a TPE molecule bonded with half of a BDTP (see below).

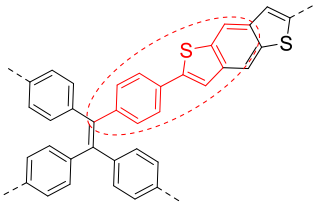

Synthesis of TPE-CMP [2]:

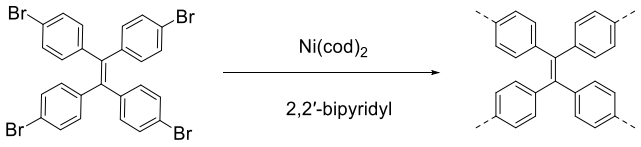

Scheme S4. Synthesis of **TPE-CMP.**

1,5-Cyclooctadiene (cod, 0.1 mL, 0.802 mmol, dried over CaH_2) was added to a solution of bis(1,5-cyclooctadiene)nickel(0) ([$Ni(cod)_2$], 221.0 mg, 0.802 mmol) and 2,2′-bipyridyl (126.0 mg, 0.802 mmol) in dehydrated DMF (15 mL), and the resulting mixture was heated at 80 °C for 1 h. Then TPE-4Br (100.0 mg, 0.154 mmol) was added to the reaction mixture, which was subsequently stirred at 80 °C for 72 h to afford a deep purple suspension. After cooling down to room temperature, concentrated HCl (4 mL) solution was added to the mixture. After filtration, the obtained precipitate was washed with H_2O, $CHCl_3$ and THF, extracted by Soxhlet with H_2O, $CHCl_3$, methanol, acetone and THF for 1 day, respectively. The obtained solid was then dried in vacuo at 100 °C for 24 h to give yellow powder (yield: 88%). The Ni metal loading of TPE-CMP was determined by ICP-AES to be 0.3%. Elemental analysis results (%) for TPE-CMP: C, 93.57; H, 5.86. The catalytically active unit of TPE-CMP is tentatively illustrated as the repeating units: one-fourth of a TPE molecule (see below).

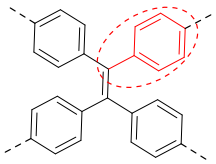

Typical Procedure for Photocatalytic Synthesis of Benzimidazoles. Photocatalyst (1-4 mg), benzene-1,2-diamine or its derivatives (0.2 mmol), aldehydes (0.2 mmol) and solvent (4.0 mL) were added into a glass bottle. The reaction mixture was opened to air and stirred at room temperature under the irradiation of 24 W blue LED (460 nm, 0.08 W/cm^2). After the reaction was completed (monitored by TLC), the catalyst was filtered from reaction mixture and thoroughly

washed by C_2H_5OH. After all the volatiles were removed under reduced pressure, the resulted crude product was further purified by flash column chromatography (petroleum/ethyl acetate = 10/1~5/1 as eluent) to give benzimidazoles.

Scale-up experiment. Benzene-1,2-diamine (540.7 mg, 5 mmol), benzaldehyde (530.6 mg, 5 mmol), PAF-366 (50.0 mg, 5.6 mol%) and C_2H_5OH (100 mL) were added into a glass bottle. The reaction mixture was opened to air and stirred at room temperature under the irradiation 24 W blue LED (460 nm, 0.08 W/cm^2). After the reaction was completed (monitored by TLC), the catalyst was filtered from reaction mixture and thoroughly washed by C_2H_5OH. After the all the volatile were removed under reduced pressure, the resulted crude product was further purified by flash column chromatography (petroleum/ethyl acetate = 10:1 as eluent). The obtained solid was then dried in vacuo at 80 °C for 12 h to give pure 2-phenyl-1H-benzo[d]imidazole (902.8 mg, 93% yield).

Recycling experiment. The catalyst is filtered out from reaction mixture and Soxhlet extracted with CH_2Cl_2 and THF for 24 h and dried in vacuo at 100 °C for 24 h. The recycled catalyst is used for a repeat catalysis experiment under the same reaction conditions.

React-IR measurement. The catalytic reaction monitored by IR probe was carried out in a three necked round-bottomed flask, equipped with a magnetic stirrer. The IR probe was inserted through an adapter into the middle neck. Reaction conditions: *o*-Phenylenediamine (0.2 mmol), benzaldehyde (0.2 mmol), PAF-366 (2 mg, 5.6 mol%), C_2H_5OH (4.0 mL), air, 24 W blue LED (460 nm, 0.08 W/cm^2), 298 K, 2 h.

Detection of H_2O_2. Sample preparation: N, N-diethyl-1,4-phenylenediammonium sulfate (DPD) reagent was prepared by dissolving 0.1 g of DPD in 10 mL 0.05 mol/L H_2SO_4 and stored in the darkness at 5 °C. Horseradish peroxidase (POD) reagent was prepared by dissolving l0 mg POD in 10 mL deionized water. The standard solution was stored at 5 °C. Both DPD and POD were prepared freshly on demand.

Typical procedure for the detection of H_2O_2: The photocatalyst PAF-366 (2 mg, 5.6 mol%), o-Phenylenediamine (0.2 mmol) and benzaldehyde (0.2 mmol) were dispersed in C_2H_5OH (4.0 mL). The reaction mixture was opened to air and stirred at room temperature under the irradiation of 24 W blue LED for 3 h. Afterwards, the resulting mixture was filtered to remove PAF-366. 20 mL deionized water was added to the obtained filtrate solution, and the mixture was further washed with ethyl acetate (20 mL × 3) to remove the organic compounds. The aqueous phase was diluted to 400 mL by adding deionized water. 9 mL aqueous solution and 1 mL PBS buffer (pH = 7.4) was mixed into the beaker and used as the test sample. The ultraviolet-visible spectra of the test sample were recorded after adding 20 μL DPD and 20 μL POD.

Pore size distribution

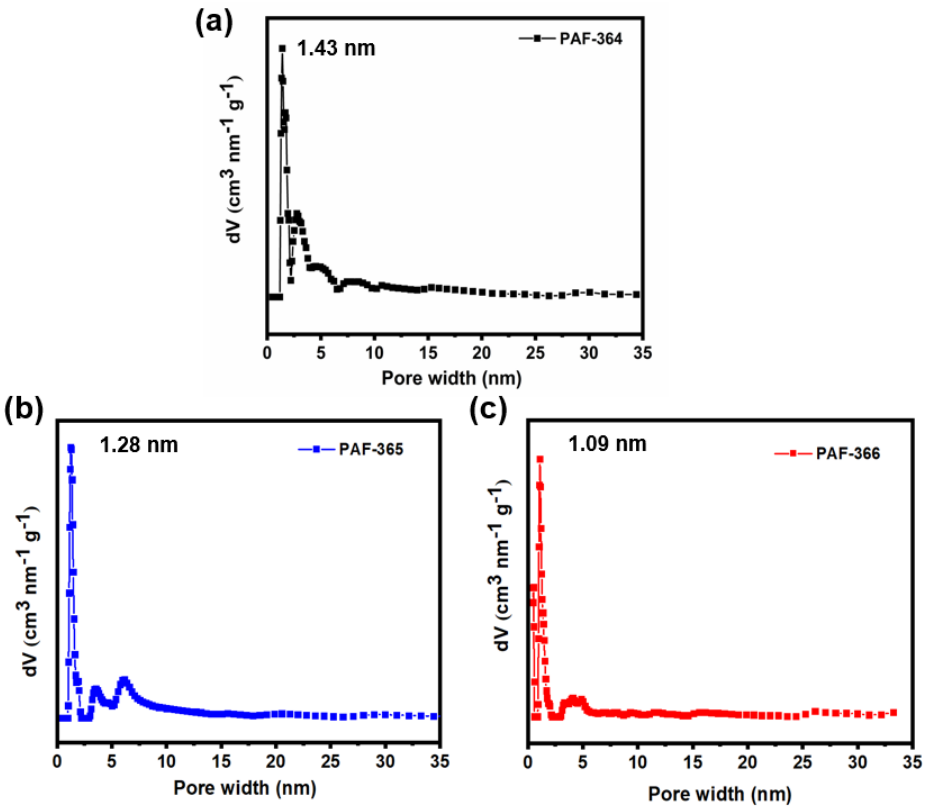

Fig. S1 Pore size distribution of PAF-364, PAF-365 and PAF-366.

XPS Spectra

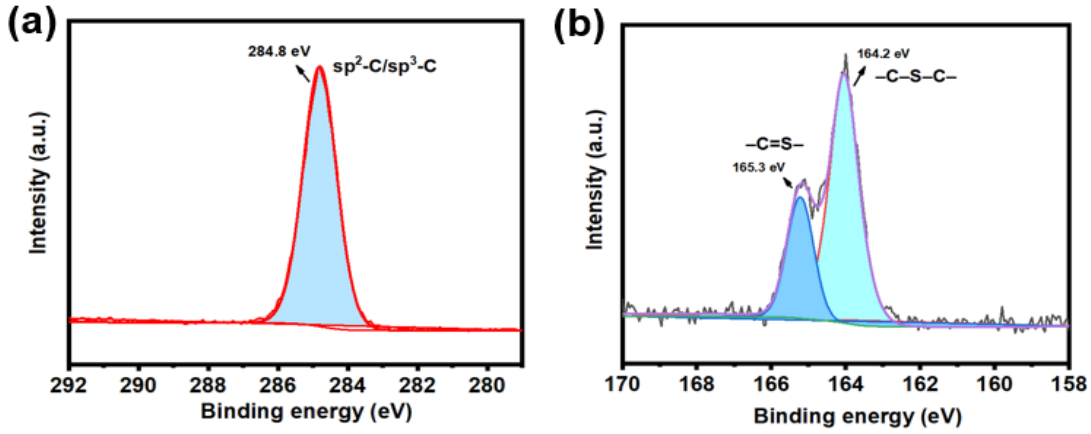

Fig. S2 XPS spectra. (a) C 1s, (b) S 2p for PAF-364.

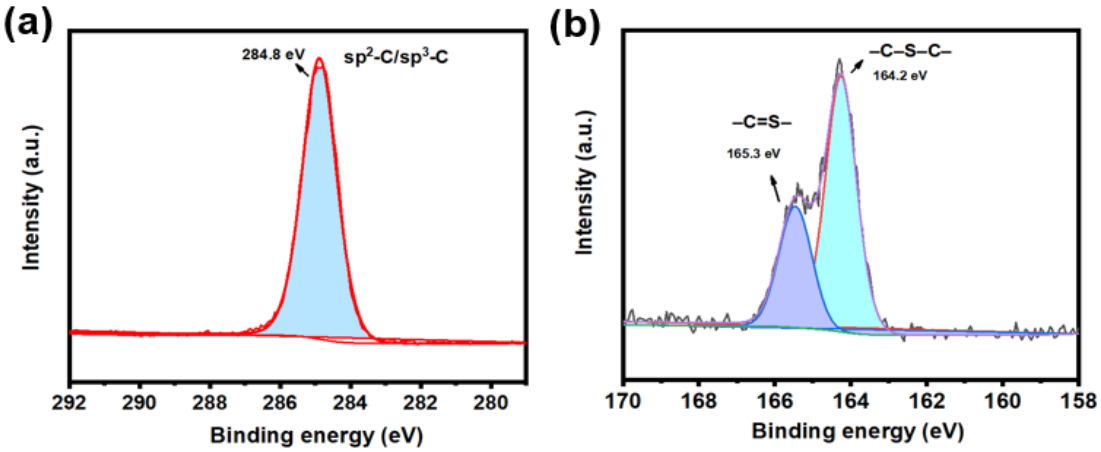

Fig. S3 XPS spectra. (a) C 1s, (b) S 2p for PAF-365.

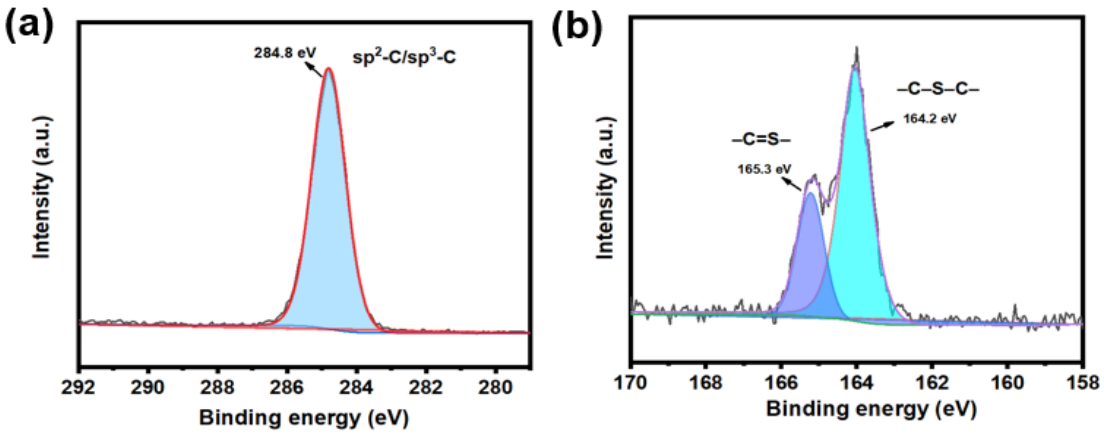

Fig. S4 XPS spectra. (a) C 1s, (b) S 2p for PAF-366.

TGA curves

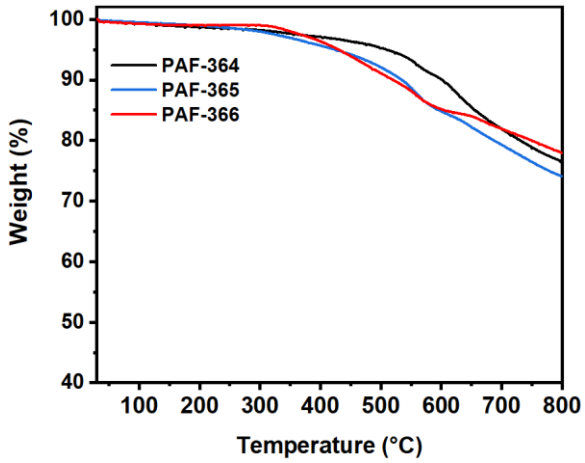

Fig. S5 TGA curves of PAF-364, PAF-365 and PAF-366.

Computational details[3]

All computations in this work are performed at the B3LYP/6-31+G (d, p) level of theory as implemented in the Gaussian 16 program.

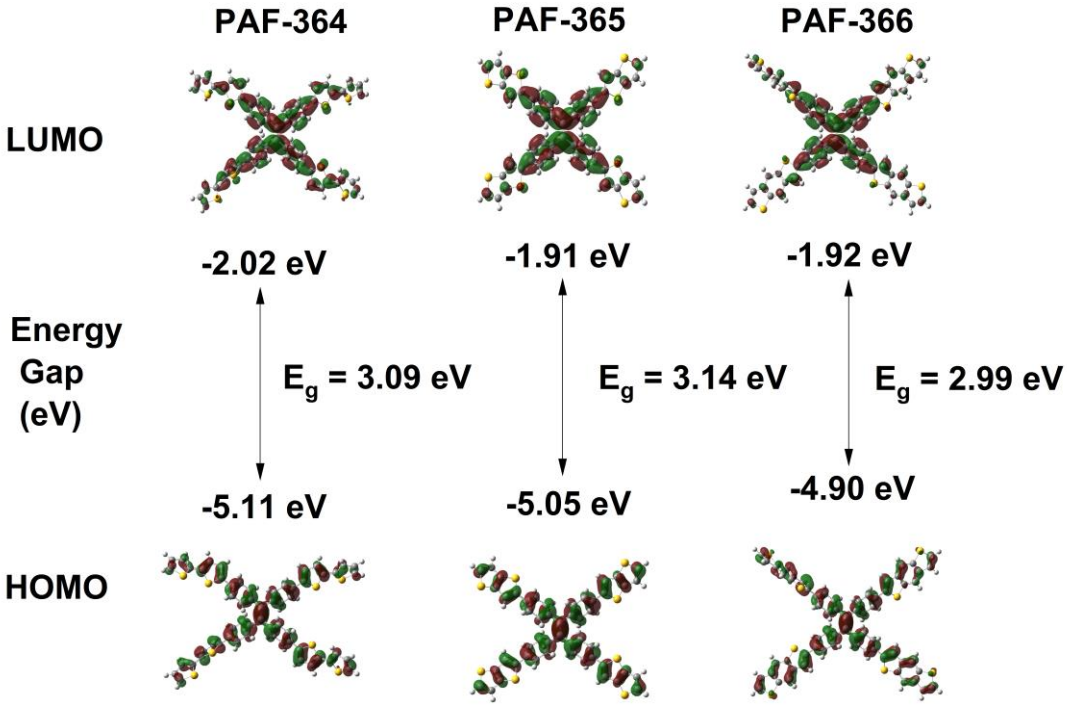

Fig. S6 The HOMO and LUMO orbital distributions of the simplified TPE-PAFs fragments from DFT simulation.

The characterizations of TPE-CMP

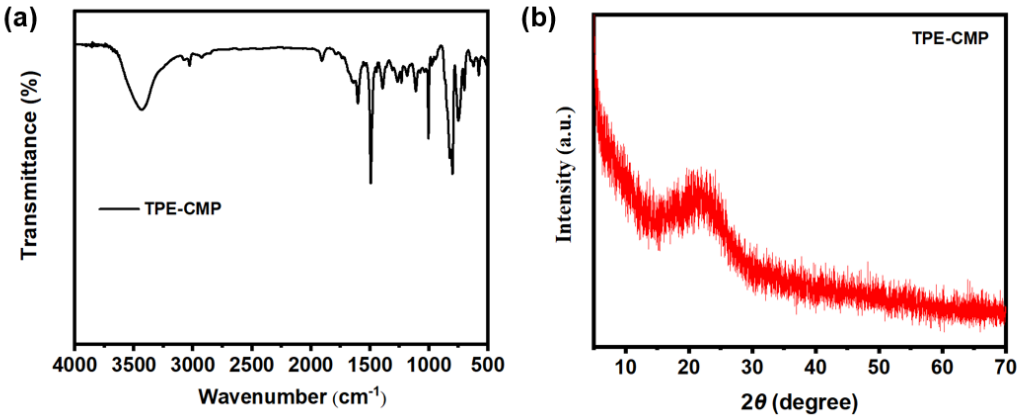

Fig. S7 (a) FT-IR spectrum and (b) PXRD pattern of TPE-CMP.

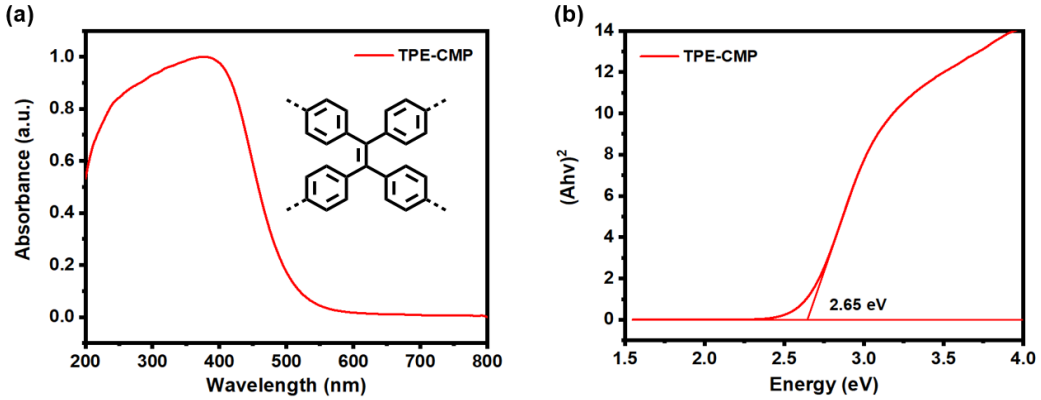

Fig. S8 (a) Solid-state absorption profile and (b) Tauc plot of TPE-CMP.

Solvent screening for the synthesis of benzimidazole

Table S1 Optimization of the reaction conditions [a].

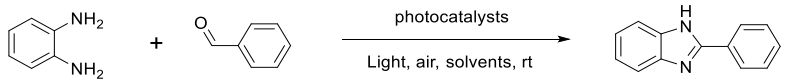

Entry	Catalyst	Amount (mg, mol%) [b]	Solvent	Yield [c] (%)
1	PAF-364	2 mg, 6.0 mol%	THF	Trace
2	PAF-364	2 mg, 6.0 mol%	toluene	9%
3	PAF-364	2 mg, 6.0 mol%	CH_3CN	28%
4	PAF-364	2 mg, 6.0 mol%	DMF	Trace
5	PAF-364	2 mg, 6.0 mol%	acetone	Trace
6	PAF-364	2 mg, 6.0 mol%	CH_2Cl_2	18%
7	PAF-364	2 mg, 6.0 mol%	1,4-dioxane	45%
8	PAF-365	2 mg, 6.5 mol%	THF	Trace
9	PAF-365	2 mg, 6.5 mol%	toluene	7%
10	PAF-365	2 mg, 6.5 mol%	CH_3CN	21%
11	PAF-365	2 mg, 6.5 mol%	DMF	Trace
12	PAF-365	2 mg, 6.5 mol%	acetone	Trace
13	PAF-365	2 mg, 6.5 mol%	CH_2Cl_2	15%
14	PAF-365	2 mg, 6.5 mol%	1,4-dioxane	39%

[a] *o*-Phenylenediamine (0.2 mmol), benzaldehyde (0.2 mmol), solvent (4 mL), air, 460 nm blue LED lamp (24 W, 0.08 W/cm^2), 298 K, 3 h. [b] The molar ratio of the repeating units of the catalysts versus substrates. [c] Isolated yields.

ESR spectra

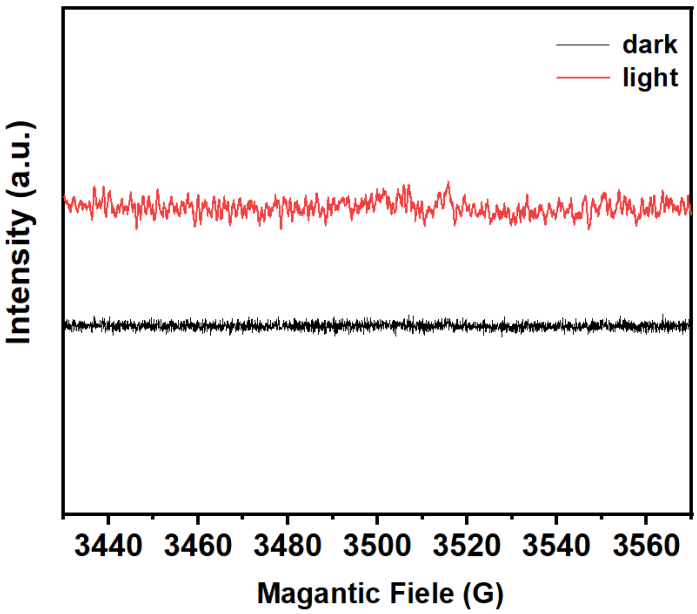

Fig. S9 ESR spectra of PAF-366 (2.0 mg mL^{-1}) and TEMP (0.1 M) in methanol under light illumination (red) and in the darkness (black).

Detection of 2-methyl-1H-benzo[d]imidazole

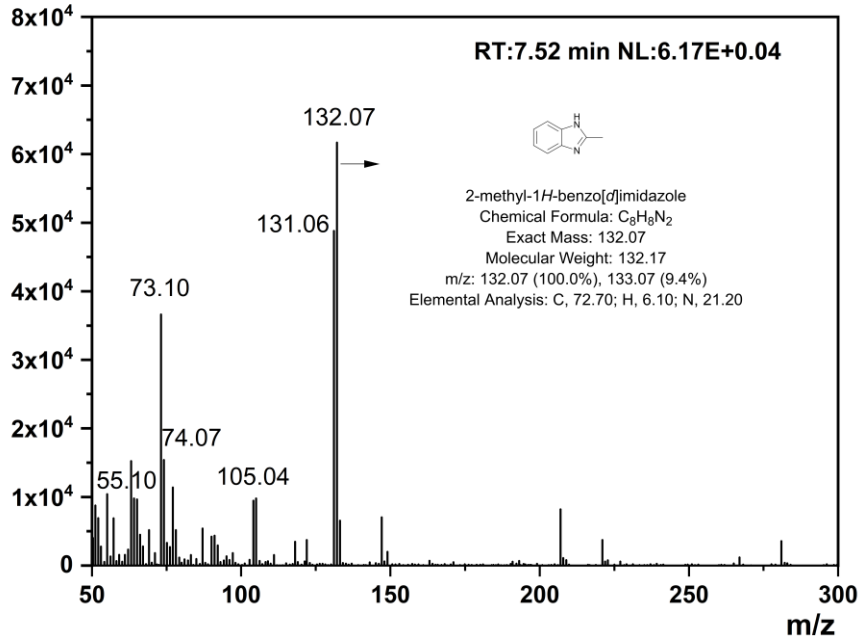

Fig. S10 GC-MS spectrum for the detection of 2-methyl-1H-benzo[d]imidazole in the reaction system. Reaction condition: C_2H_5OH (4 mL), PAF-366 (2 mg, 5.6 mol%), o-phenylenediamine (0.2 mmol), benzaldehyde (0.2 mmol), rt, 460 nm blue LED light (24 W, 0.08 W/cm^2), air, 3h.

Scale-up experiment for the synthesis of 2-phenyl-1H-benzo[d]imidazole

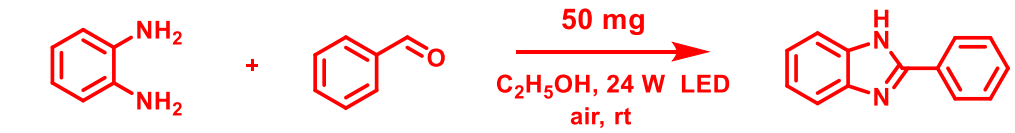

5 mmol, 540.7 mg 5 mmol, 530.6 mg 5 mmol, 971.2 mg

5 h, 902. 8 mg, yield 93%

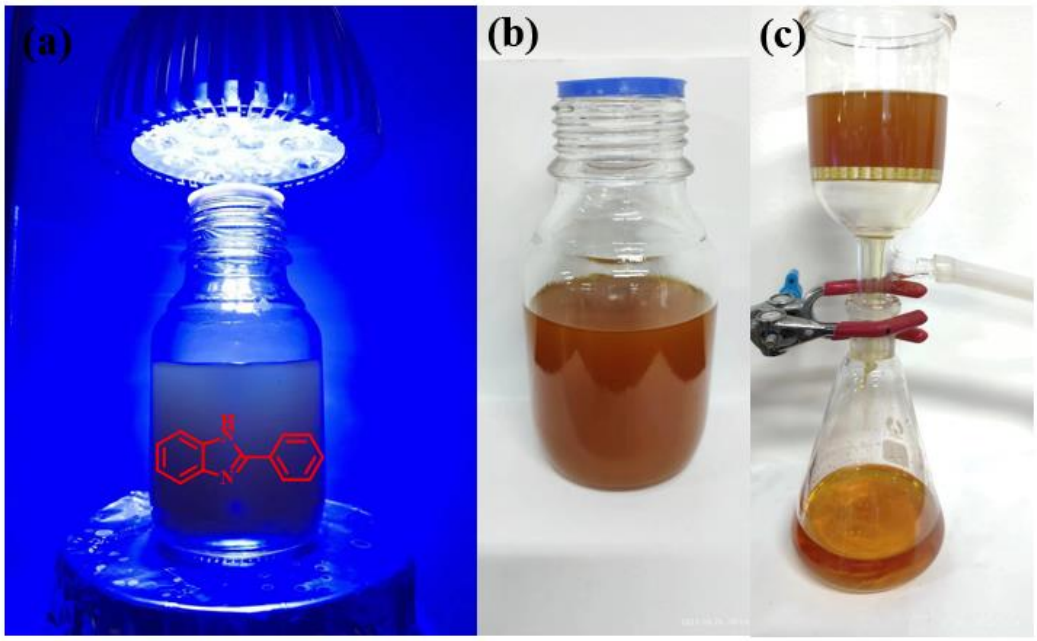

Fig. S11 Scale-up experiment of 2-phenyl-1H-benzo[d]imidazole with PAF-366 as photocatalyst. (a) Photocatalytic reaction equipment. (b) The completed reaction system that contain product 2-phenyl-1H-benzo[d]imidazole and PAF-366; (c) Recycling of PAF-366 through filtration.

Recyclability tests of PAF-366

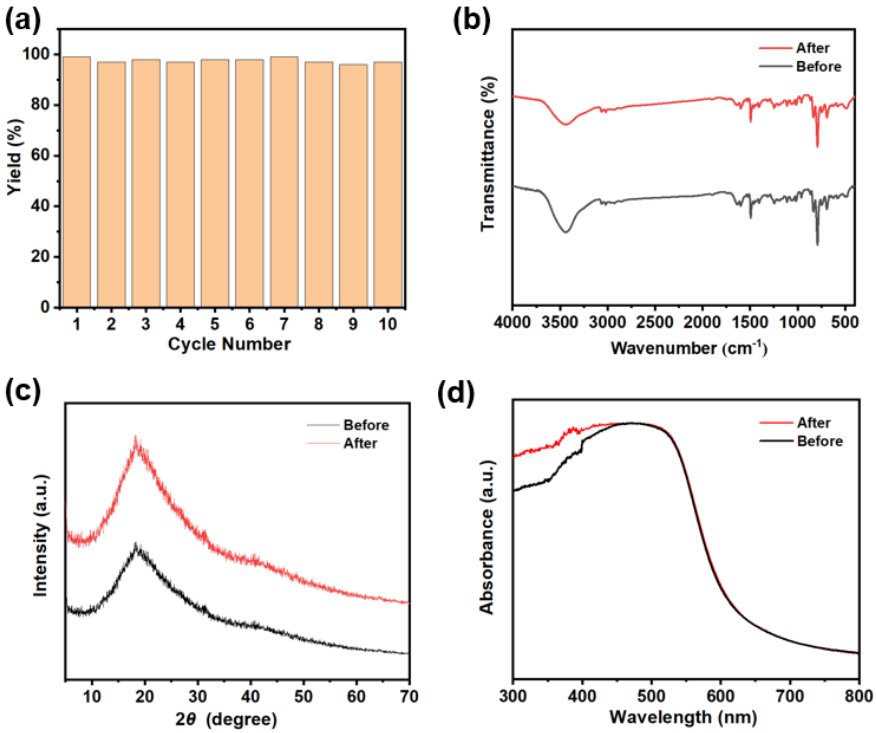

Fig. S12 (a) Reusability of PAF-366 in the photocatalytic synthesis of 2-phenyl-1H-benzo[d]imidazole. (b) FT-IR spectra, (c) PXRD patterns and (d) Solid-state absorption profiles of photocatalyst PAF-366 in the first and tenth cycles.

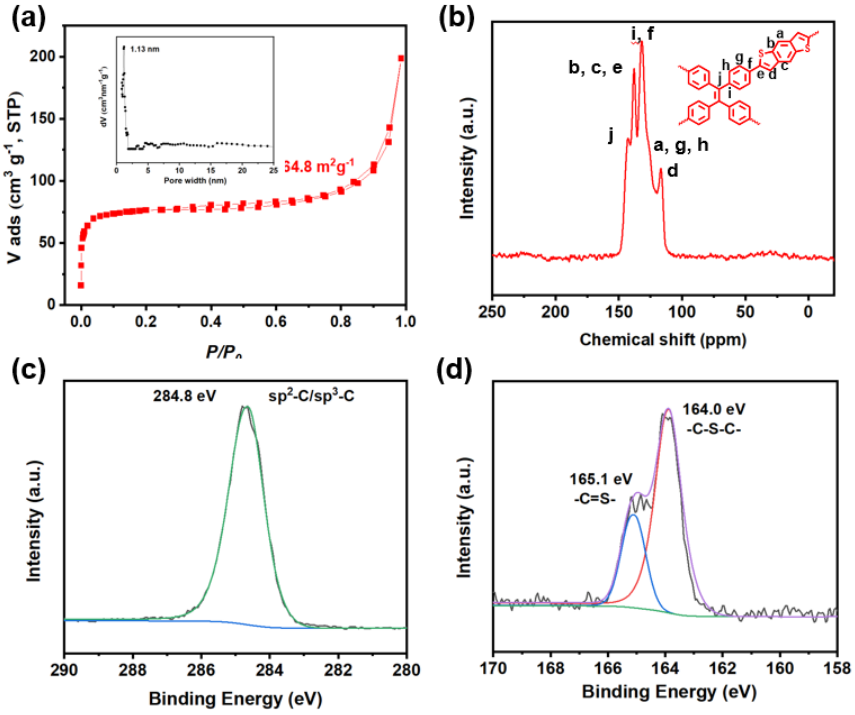

Fig. S13 (a) N_2 adsorption/desorption isotherms at 77 K (b) ^{13}C CP-MAS Solid-state NMR spectrum. The XPS spectra of C 1s (c) and S 2p (d) for PAF-366 after ten cycles.

Liquid NMR Spectra

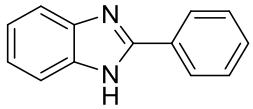

2-phenyl-1H-benzo[d]imidazole (3a): White solid. **^{1}H NMR** (500 MHz, DMSO-d_6) δ 12.93 (s, 1H), 8.21 (d, *J* = 8.5 Hz, 2H), 7.68-7.48 (m, 5H), 7.22 (dd, *J* = 6.0, 3.1 Hz, 2H) ppm. **^{13}C NMR** (126 MHz, DMSO-d_6) δ 151.7, 130.7, 130.3, 129.4, 126.9, 122.5 ppm.

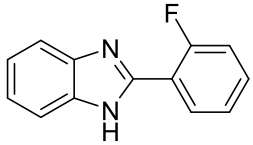

2-(2-fluorophenyl)-1H-benzo[d]imidazole (3b): White solid. **^{1}H NMR** (500 MHz, DMSO-d_6) δ 12.59 (s, 1H), 8.25 (td, *J* = 7.8, 1.6 Hz, 1H), 7.70 (s, 1H), 7.65-7.54 (m, 2H), 7.50-7.37 (m, 2H), 7.24 (d, *J* = 3.6 Hz, 2H) ppm. **^{13}C NMR** (126 MHz, DMSO-d_6) δ160.7, 158.7, 146.9, 146.9, 143.5, 135.5, 132.3 (d, *J* = 8.6 Hz), 130.7 (d, *J* = 2.6 Hz), 125.5 (d, *J* = 3.0 Hz), 123.0, 119.4, 118.5 (d, *J* = 11.2 Hz), 117.1, 116.9 (d, *J* = 21.8 Hz), 112.4 ppm.

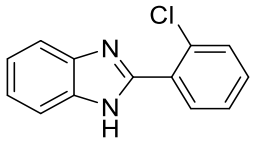

2-(2-chlorophenyl)-1H-benzo[d]imidazole (3c): White solid. **^{1}H NMR** (500 MHz, DMSO-d_6) 12.74 (s, 1H), 7.93 (dd, *J* = 7.2, 2.2 Hz, 1H), 7.72 (s, 1H), 7.66 (dd, *J* = 7.6, 1.5 Hz, 1H), 7.59 (s, 1H), 7.57 – 7.49 (m, 2H), 7.25 (s, 2H) ppm. **^{13}C NMR** (126 MHz, DMSO-d_6) δ 149.6, 143.8, 135.4, 132.6, 132.1, 131.7, 130.9, 130.5, 127.8, 123.2, 122.2, 119.6, 112.2 ppm.

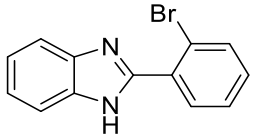

2-(2-bromophenyl)-1H-benzo[d]imidazole (3d): White solid. **^{1}H NMR** (500 MHz, DMSO-d_6) δ 13.07 (s, 1H), 8.41 (s, 1H), 8.23 (d, *J* = 7.7 Hz, 1H), 7.72 (d, *J* = 7.4 Hz, 2H), 7.66 – 7.50 (m, 2H), 7.38 – 7.19 (m, 2H) ppm. **^{13}C NMR** (126 MHz, DMSO-d_6) δ 150.0, 144.1, 135.4, 132.9, 131.8, 129.5, 125.8, 123.4, 122.7, 122.4, 119.4, 112.2 ppm.

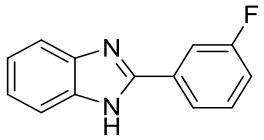

2-(3-fluorophenyl)-1H-benzo[d]imidazole (3e): White solid. **^{1}H NMR** (500 MHz, DMSO-d_6) δ 13.00 (s, 1H), 8.03 (d, *J* = 7.8 Hz, 1H), 7.96 (dd, *J* = 7.1, 4.8 Hz, 1H), 7.71 – 7.53 (m, 3H), 7.34 (td, *J* = 8.4, 2.4 Hz, 1H), 7.23 (dt, *J* = 15.0, 6.7 Hz, 2H) ppm. **^{13}C NMR** (126 MHz, DMSO-d_6) 163.9, 162.0, 150.4, 144.1, 135.3, 133.1 (d, *J* = 8.2 Hz), 131.7 (d, *J* = 8.1 Hz), 123.4, 123.0 (d, *J* = 2.6 Hz), 122.4, 119.7, 117.1(d, *J* = 21.0 Hz), 113.4 (d, *J* = 23.5 Hz), 112.0 ppm.

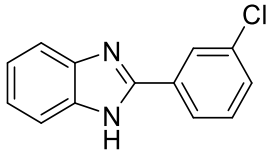

2-(3-chlorophenyl)-1H-benzo[d]imidazole (3f): White solid. **^{1}H NMR** (500 MHz, DMSO-d_6) δ 13.05 (s, 1H), 8.25 (s, 1H), 8.17 (d, *J* = 7.5 Hz, 1H), 7.70 (s, 1H), 7.64 – 7.54 (m, 3H), 7.25 (s, 2H) ppm. **^{13}C NMR** (126 MHz, DMSO-d_6) δ 150.3, 144.2, 135.6, 134.3, 132.6, 131.2, 130.0, 126.3, 125.6, 123.3, 122.4, 119.6, 112.0 ppm.

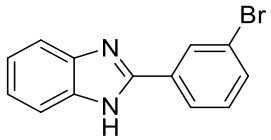

2-(3-bromophenyl)-1H-benzo[d]imidazole (3g): White solid. **^{1}H NMR** (500 MHz, DMSO-d_6) δ 13.06 (s, 1H), 8.41 (t, *J* = 1.6 Hz, 1H), 8.22 (d, *J* = 7.9 Hz, 1H), 7.70 (dd, *J* = 7.9, 1.0 Hz, 2H), 7.66 – 7.48 (m, 2H), 7.35 – 7.15 (m, 2H) ppm. **^{13}C NMR** (126 MHz, DMSO-d_6) δ 150.1, 144.1, 135.5, 132.9, 131.6, 129.3, 125.9, 123.49, 122.6, 119.6, 112.0 ppm.

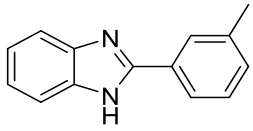

2-(m-tolyl)-1H-benzo[d]imidazole (3h): Light yellow solid. **^{1}H NMR** (500 MHz, DMSO-d_6) δ 12.87 (s, 1H), 8.05 (s, 1H), 7.99 (d, *J* = 7.8 Hz, 1H), 7.67 (d, *J* = 7.1 Hz, 1H), 7.54 (d, *J* = 7.0 Hz, 1H), 7.45 (t, *J* = 7.6 Hz, 1H), 7.32 (d, *J* = 7.5 Hz, 1H), 7.22 (d, *J* = 7.9 Hz, 2H), 2.43 (s, 3H) ppm. **^{13}C NMR** (126 MHz, DMSO-d_6) δ 151.8, 144.2, 138.6, 135.6, 131.0, 129.2, 127.5, 124.0, 122.9, 122.1, 119.2, 111.8, 21.5 ppm.

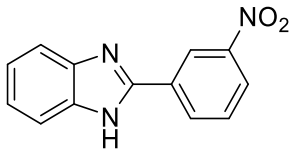

2-(3-nitrophenyl)-1H-benzo[d]imidazole (3i): Light yellow solid. **^{1}H NMR** (500 MHz, DMSO-d_6) δ 13.35 (s, 1H), 9.07 (s, 1H), 8.67 (d, *J* = 7.9 Hz, 1H), 8.46 – 8.32 (m, 1H), 7.91 (t, *J* = 8.0 Hz, 1H), 7.71 (s, 2H), 7.31 (dd, *J* = 5.7, 2.8 Hz, 2H) ppm. **^{13}C NMR** (126 MHz, DMSO-d_6) δ 149.5, 148.9, 133.0, 132.2, 131.2, 124.8, 121.3 ppm.

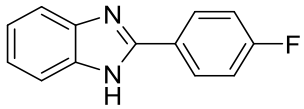

2-(4-fluorophenyl)-1H-benzo[d]imidazole (3j): White solid. **^{1}H NMR** (500 MHz, DMSO-d_6) δ 12.90 (s, 1H), 8.22 (d, *J* = 14.2 Hz, 2H), 7.66 (d, *J* = 7.6 Hz, 1H), 7.53 (d, *J* = 7.4 Hz, 1H), 7.40 (t, *J* = 8.8 Hz, 2H), 7.24 – 7.07 (m, 2H) ppm. **^{13}C NMR** (126 MHz, DMSO-d_6) δ 162.5, 150.8, 144.3, 135.5, 129.2 (d, *J* = 8.7 Hz), 127.3 (d, *J* = 2.9 Hz), 123.0, 122.2, 119.3, 116.5 (d, J = 21.9 Hz), 111.8 ppm.

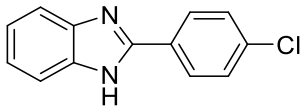

2-(4-chlorophenyl)-1H-benzo[d]imidazole (3k): White solid. **^{1}H NMR** (500 MHz, DMSO-d_6) δ 12.98 (s, 1H), 8.20 (d, *J* = 8.6 Hz, 2H), 7.68 (d, *J* = 7.6 Hz, 1H), 7.64 (d, *J* = 8.5 Hz, 2H), 7.55 (d, *J* = 7.4 Hz, 1H), 7.28 – 7.14 (m, 2H) ppm. **^{13}C NMR** (126 MHz, DMSO-d_6) δ ^{13}C NMR (126 MHz, DMSO-d_6) δ 150.5, 144.2, 135.5, 129.7, 128.6, 123.2, 122.2, 119.4, 111.9 ppm.

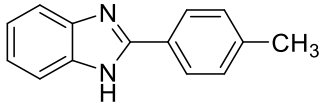

2-(p-tolyl)-1H-benzo[d]imidazole (3l): Light yellow solid. **^{1}H NMR** (500 MHz, DMSO-d_6) δ 12.86 (s, 1H), 8.12 (d, *J* = 8.1 Hz, 2H), 7.69 (d, *J* = 7.6 Hz, 1H), 7.56 (d, *J* = 7.5 Hz, 1H), 7.41 (d, *J* = 8.0 Hz, 2H), 7.33 – 7.14 (m, 2H), 2.43 (s, 3H) ppm. **^{13}C NMR** (126 MHz, DMSO-d_6) δ 152.0, 144.4, 140.1, 135.7, 130.2, 127.7, 126.6, 122.9, 121.9, 119.2, 111.7, 21.30 ppm.

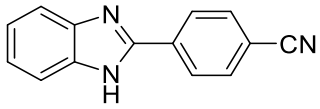

4-(1H-benzo[d]imidazol-2-yl)benzonitrile (3m): Light yellow solid. **^{1}H NMR** (500 MHz, DMSO-d_6) δ 13.20 (s, 1H), 8.36 (d, *J* = 8.3 Hz, 2H), 8.03 (d, *J* = 8.3 Hz, 2H), 7.67 (d, *J* = 49.3 Hz, 2H), 7.28 (s, 2H) ppm. **^{13}C NMR** (126 MHz, DMSO-d_6) δ 150.2, 144.1, 135.7, 134.8, 133.5, 127.2, 123.9, 122.5, 119.9, 118.7, 112.2 ppm.

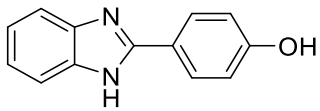

4-(1H-benzo[d]imidazol-2-yl)phenol (3n): Light yellow solid. **^{1}H NMR** (500 MHz, DMSO-d_6) δ 12.63 (s, 1H), 9.95 (s, 1H), 7.98 (d, *J* = 8.6 Hz, 2H), 7.51 (s, 2H), 7.13 (dd, *J* = 5.8, 3.1 Hz, 2H), 6.89 (d, *J* = 8.6 Hz, 2H) ppm. **^{13}C NMR** (126 MHz, DMSO-d_6) δ 159.6, 152.3, 128.6, 121.9, 116.2 ppm.

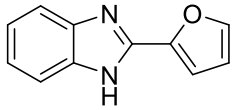

2-(thiophen-3-yl)-1H-benzo[d]imidazole (3o): Light yellow solid. **^{1}H NMR** (500 MHz, DMSO-d_6) δ 12.95 (s, 1H), 7.96 (s, 1H), 7.59 (d, *J* = 62.5 Hz, 2H), 7.23 (d, *J* = 3.1 Hz, 3H), 6.75 (s, 1H) ppm. **^{13}C NMR** (126 MHz, DMSO-d_6) δ 146.0, 145.1, 144.1, 134.7, 123.1, 122.4, 119.3, 112.9, 111.8, 110.9 ppm.

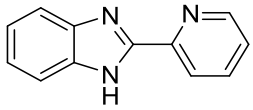

2-(pyridin-2-yl)-1H-benzo[d]imidazole (3p): White solid. **^{1}H NMR** (500 MHz, DMSO-d_6) δ 13.12 (s, 1H), 8.74 (d, *J* = 4.4 Hz, 1H), 8.36 (d, *J* = 7.9 Hz, 1H), 8.01 (td, *J* = 7.8, 1.6 Hz, 1H), 7.74 (d, *J* = 7.8 Hz, 1H), 7.57 (d, *J* = 7.7 Hz, 1H), 7.53 (dd, *J* = 7.0, 5.3 Hz, 1H), 7.22-7.28 (m, *J* = 15.1, 6.8 Hz, 2H) ppm. **^{13}C NMR** (126 MHz, DMSO-d_6) δ 151.2, 149.8, 149.0, 144.4, 138.0, 135.4, 125.2, 123.6, 122.4, 121.9, 119.8, 112.6 ppm.

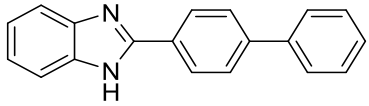

2-([1,1'-biphenyl]-4-yl)-1H-benzo[d]imidazole (3q): Light yellow solid.**^{1}H NMR** (500 MHz, DMSO-d_6) δ 12.95 (s, 1H), 8.27 (d, *J* = 8.4 Hz, 2H), 7.88 (d, *J* = 8.4 Hz, 2H), 7.78 (d, *J* = 7.4 Hz, 2H), 7.68 (d, *J* = 7.5 Hz, 1H), 7.57 – 7.48 (m, 3H), 7.41 (t, *J* = 7.3 Hz, 1H), 7.27 – 7.15 (m, 2H) ppm. **^{13}C NMR** (126 MHz, DMSO-d_6) δ 151.4, 141.8, 139.7, 129.6, 129.5, 128.4, 127.6, 127.5, 127.2, 123.1, 122.2, 119.3, 111.7 ppm.

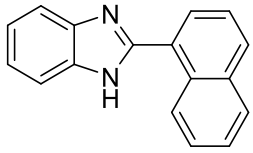

2-(naphthalen-1-yl)-1H-benzo[d]imidazole (3r): Light yellow solid. **^{1}H NMR** (500 MHz, DMSO-d_6) δ 12.92 (s, 1H), 9.11 (d, *J* = 8.4 Hz, 1H), 8.10 (d, *J* = 8.2 Hz, 1H),

8.08 – 7.99 (m, 2H), 7.78 (d, *J* = 7.6 Hz, 1H), 7.73 – 7.56 (m, 4H), 7.26 (t, *J* = 15.8 Hz, 2H) ppm. **^{13}C NMR** (126 MHz, DMSO-d_6) δ 151.8, 144.4, 134.9, 134.1, 131.0, 130.7, 128.9, 128.4, 128.0, 127.6, 126.8, 125.8, 123.2, 122.1, 119.5, 111.8 ppm.

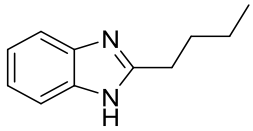

2-butyl-1H-benzo[d]imidazole (3s): White solid. **^{1}H NMR** (500 MHz, DMSO-d_6) δ 12.14 (s, 1H), 7.45 (s, 2H), 7.10 (dd, *J* = 5.7, 3.0 Hz, 2H), 2.80 (t, *J* = 7.5 Hz, 2H), 1.90 – 1.70 (m, 2H), 1.54 – 1.28 (m, 2H), 0.91 (t, *J* = 7.4 Hz, 3H) ppm. **^{13}C NMR** (126 MHz, DMSO-d_6) δ 155.6, 121.6, 30.3, 28.8, 22.7, 14.3 ppm.

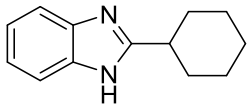

2-cyclohexyl-1H-benzo[d]imidazole (3t): Light yellow solid. **^{1}H NMR** (500 MHz, DMSO-d_6) δ 12.08 (s, 1H), 7.45 (dd, *J* = 59.7, 6.8 Hz, 2H), 7.21 – 7.00 (m, 2H), 2.92 – 2.73 (m, 1H), 2.02 (dd, *J* = 13.1, 2.7 Hz, 2H), 1.85 – 1.75 (m, 2H), 1.74 – 1.67 (m, 1H), 1.61 (dd, *J* = 27.6, 12.5 Hz, 2H), 1.46 – 1.32 (m, 2H), 1.32 – 1.21 (m, 1H) ppm. **^{13}C NMR** (126 MHz, DMSO-d_6) δ 159.3, 143.6, 134.6, 122.0, 121.2, 118.7, 111.1, 38.2, 31.7, 26.1 ppm.

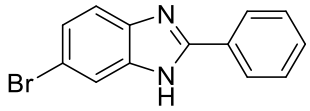

6-bromo-2-phenyl-1H-benzo[d]imidazole (3u): Light yellow solid. **^{1}H NMR** (500 MHz, DMSO-d_6) δ 13.14 (s, 1H), 8.20 (d, *J* = 7.2 Hz, 2H), 7.81 (d, *J* = 86.8 Hz, 1H), 7.68 – 7.50 (m, 4H), 7.37 (s, 1H) ppm. **^{13}C NMR** (126 MHz, DMSO-d_6) δ 152.9, 146.5, 130.7, 130.0, 129.5, 127.1, 125.2, 114.9 ppm.

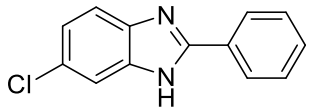

6-chloro-2-phenyl-1H-benzo[d]imidazole (3v): Light yellow solid. **^{1}H NMR** (500 MHz, DMSO-d_6) δ 13.14 (s, 1H), 8.21 (d, *J* = 7.2 Hz, 2H), 7.63 (dd, *J* = 46.7, 39.6 Hz, 4H), 7.54 (t, *J* = 7.2 Hz, 1H), 7.26 (d, *J* = 8.2 Hz, 1H) ppm. **^{13}C NMR** (126 MHz, DMSO-d_6) δ 151.9, 129.5, 129.0, 128.3, 125.9, 121.8, 119.6, 117.4, 112.0, 110.3 ppm.

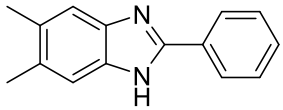

5,6-dimethyl-2-phenyl-1H-benzo[d]imidazole (3w): Light yellow solid. **^{1}H NMR**

(500 MHz, DMSO-d_6) δ 12.65 (s, 1H), 8.17 (d, J = 7.8 Hz, 2H), 7.53 (t, J = 7.5 Hz, 2H), 7.46 (t, J = 7.3 Hz, 2H), 7.31 (s, 1H), 2.33 (s, 6H) ppm. **^{13}C NMR** (126 MHz, DMSO-d_6) δ 150.8, 143.0, 134.0, 131.6, 131.0, 129.2, 111.8 ppm.

^{1}H and ^{13}C Spectra of compound 3a (DMSO)

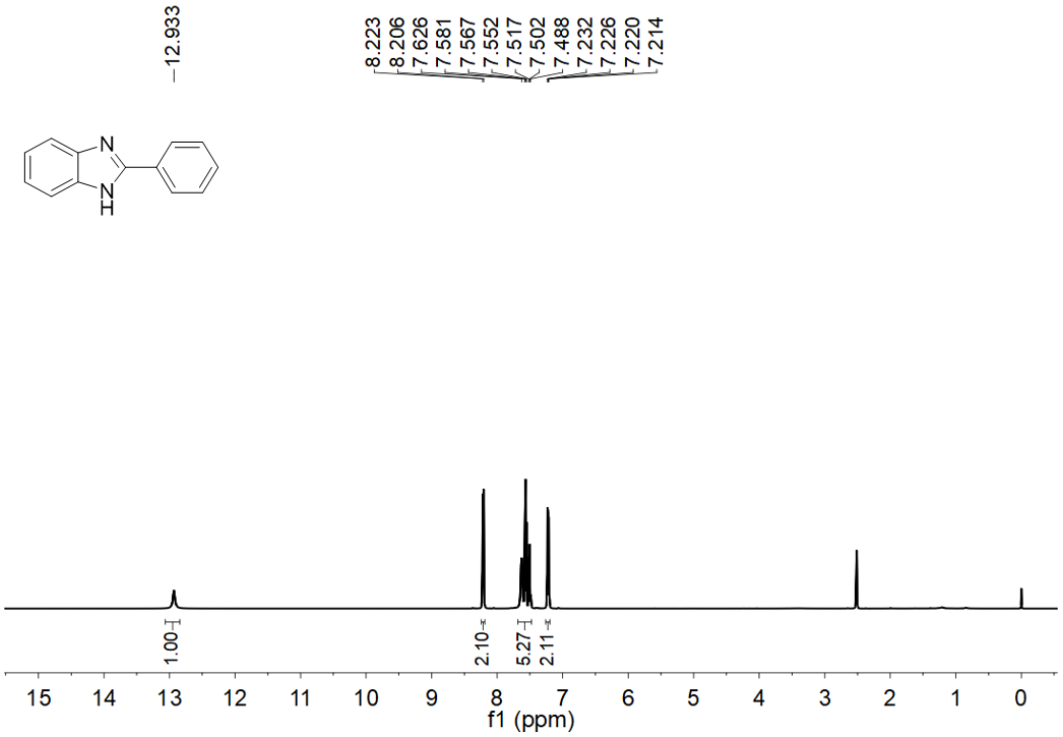

Fig. S14 ^{1}H NMR of 3a in DMSO.

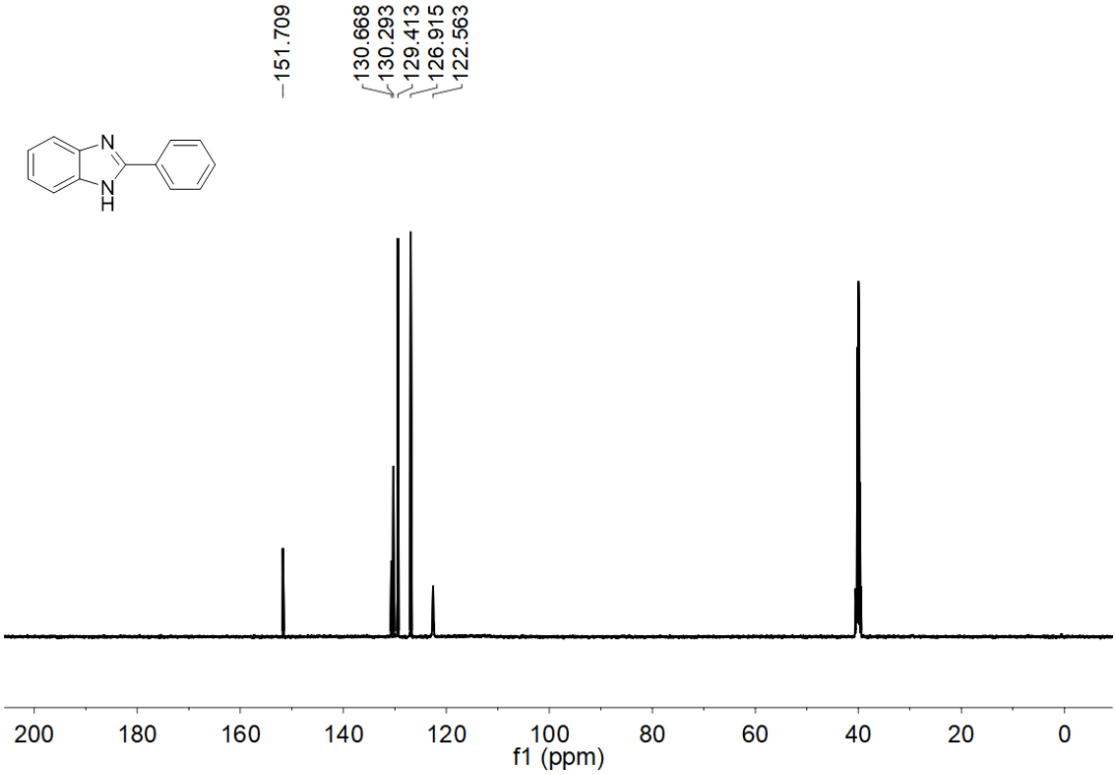

Fig. S15 ^{13}C NMR of 3a in DMSO.

^{1}H and ^{13}C Spectra of compound 3b (DMSO)

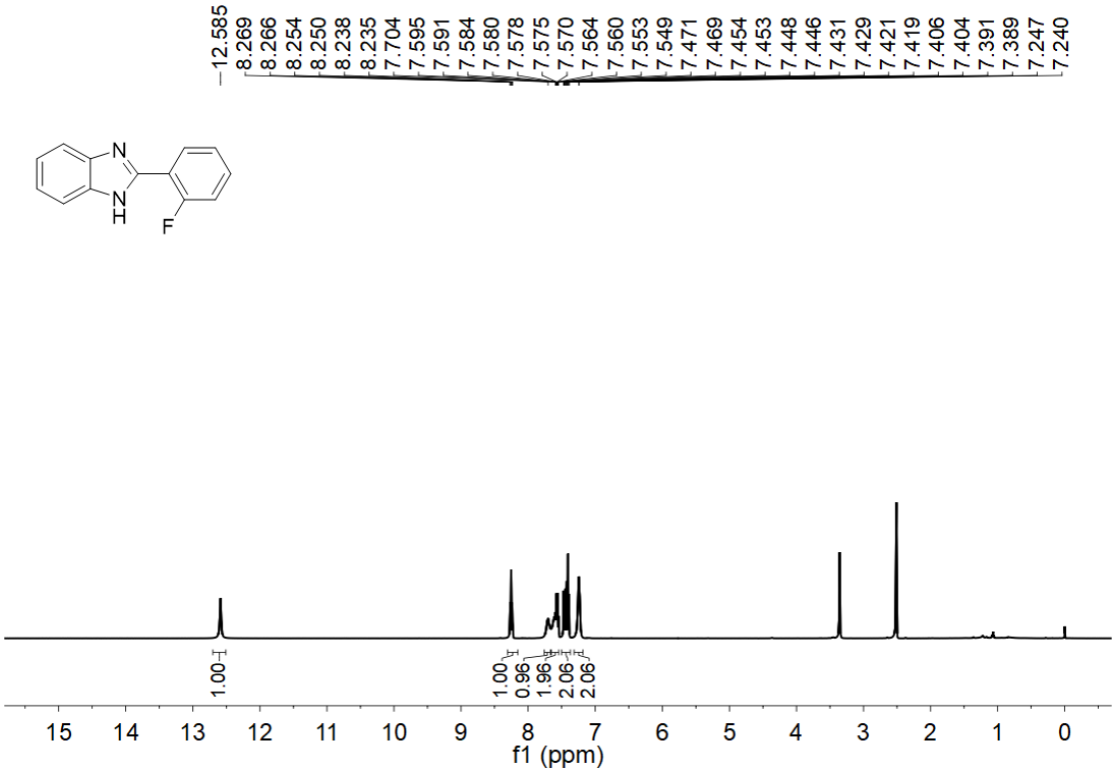

Fig. S16 ^{1}H NMR of 3b in DMSO.

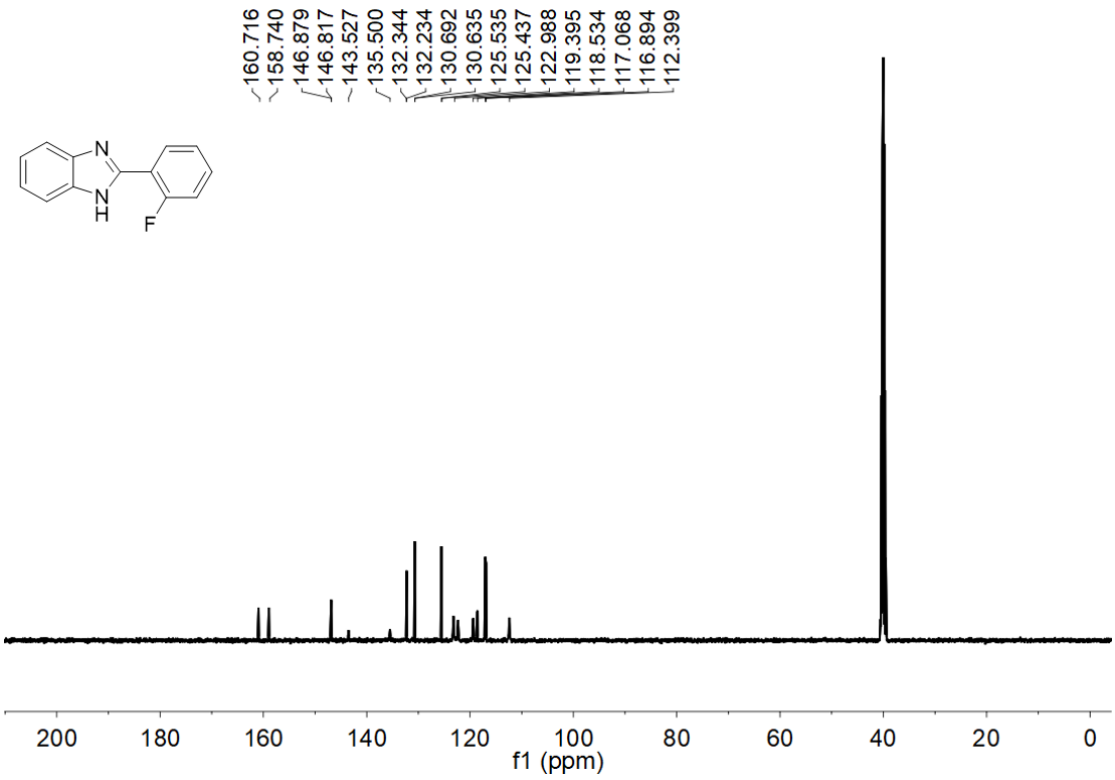

Fig. S17 ^{13}C NMR of 3b in DMSO.

^{1}H and ^{13}C Spectra of compound 3c (DMSO)

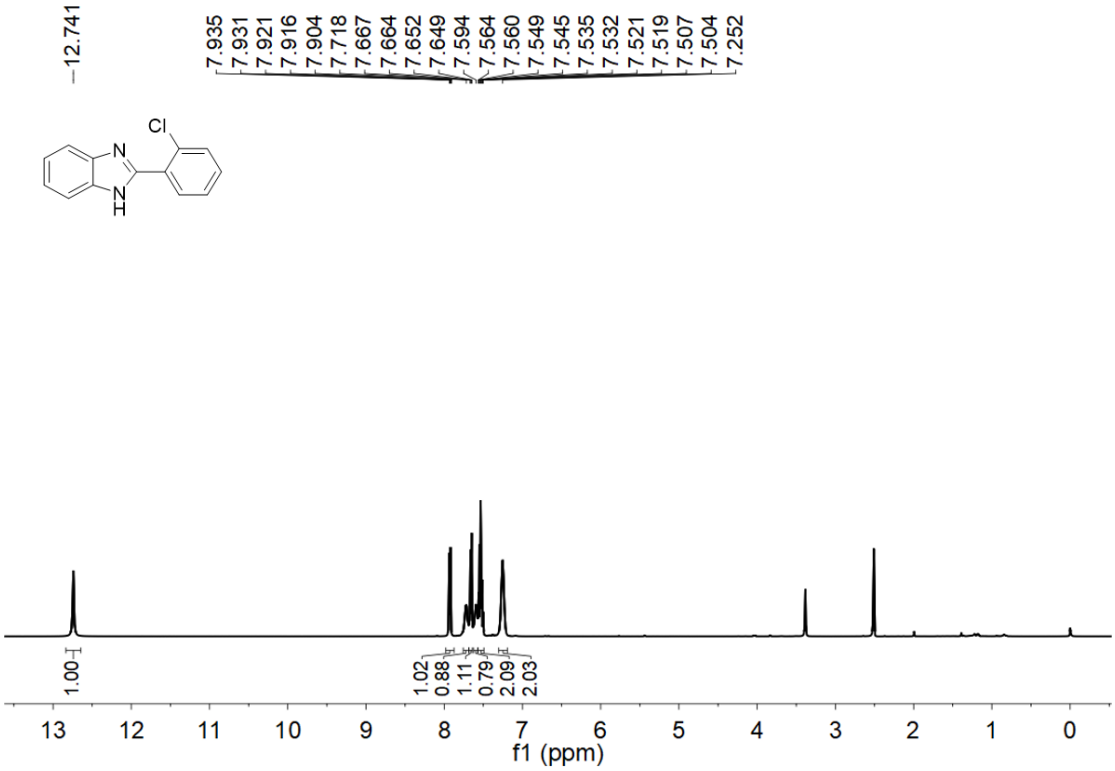

Fig. S18 ^{1}H NMR of 3c in DMSO.

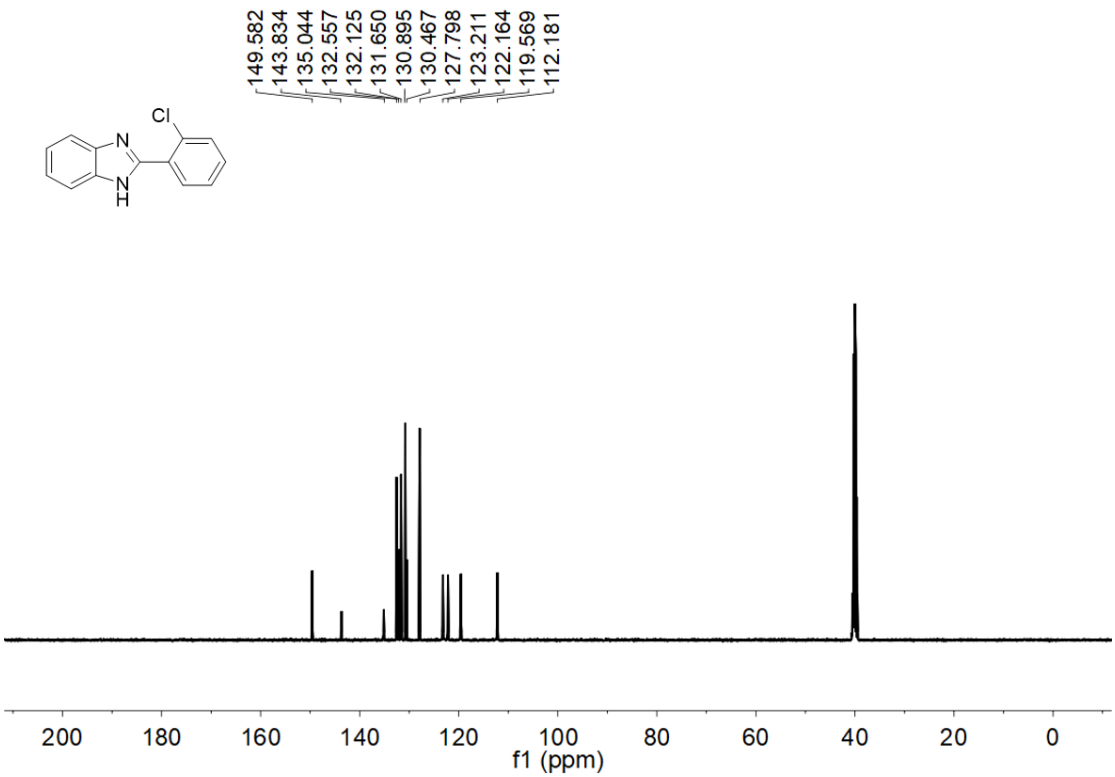

Fig. S19 ^{13}C NMR of 3c in DMSO.

^{1}H and ^{13}C Spectra of compound 3d (DMSO)

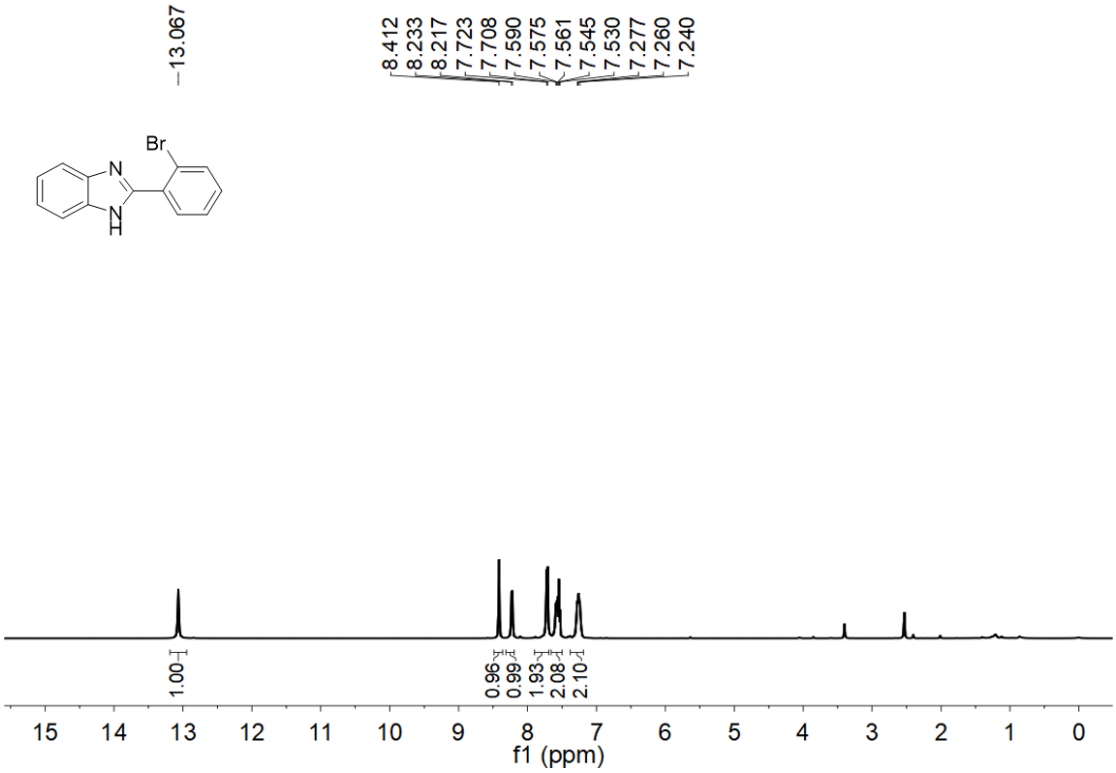

Fig. S20 ^{1}H NMR of 3d in DMSO.

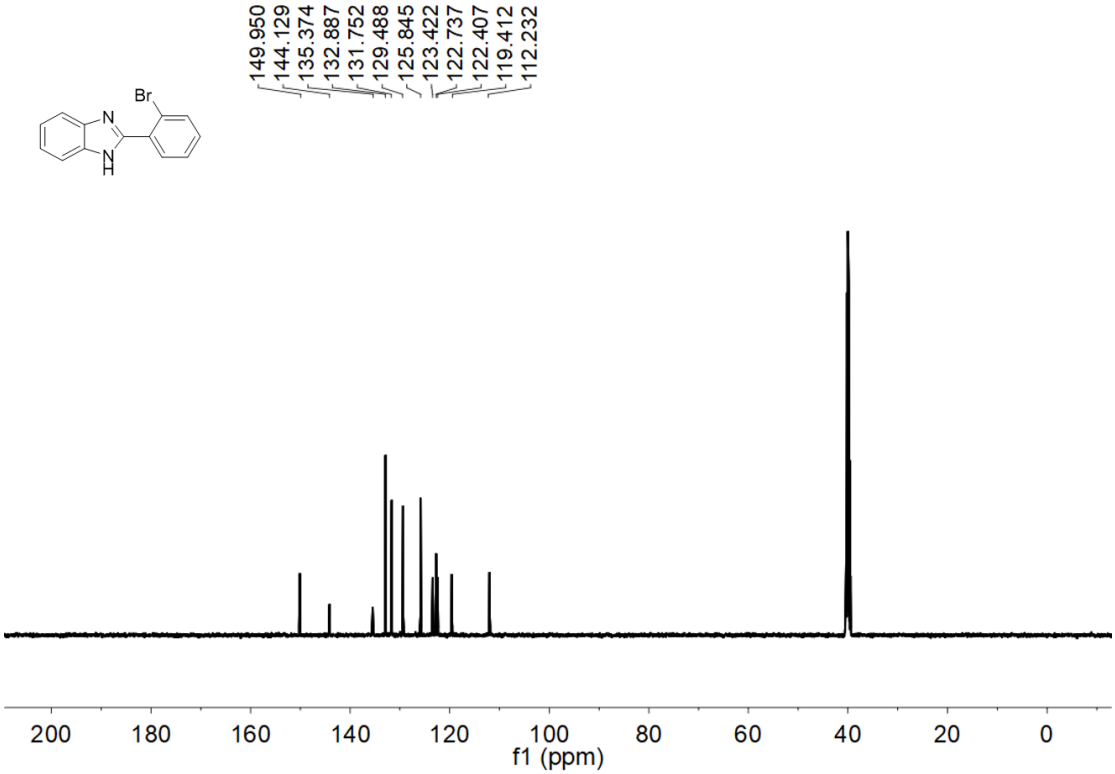

Fig. S21 ^{13}C NMR of 3d in DMSO.

^{1}H and ^{13}C Spectra of compound 3e (DMSO)

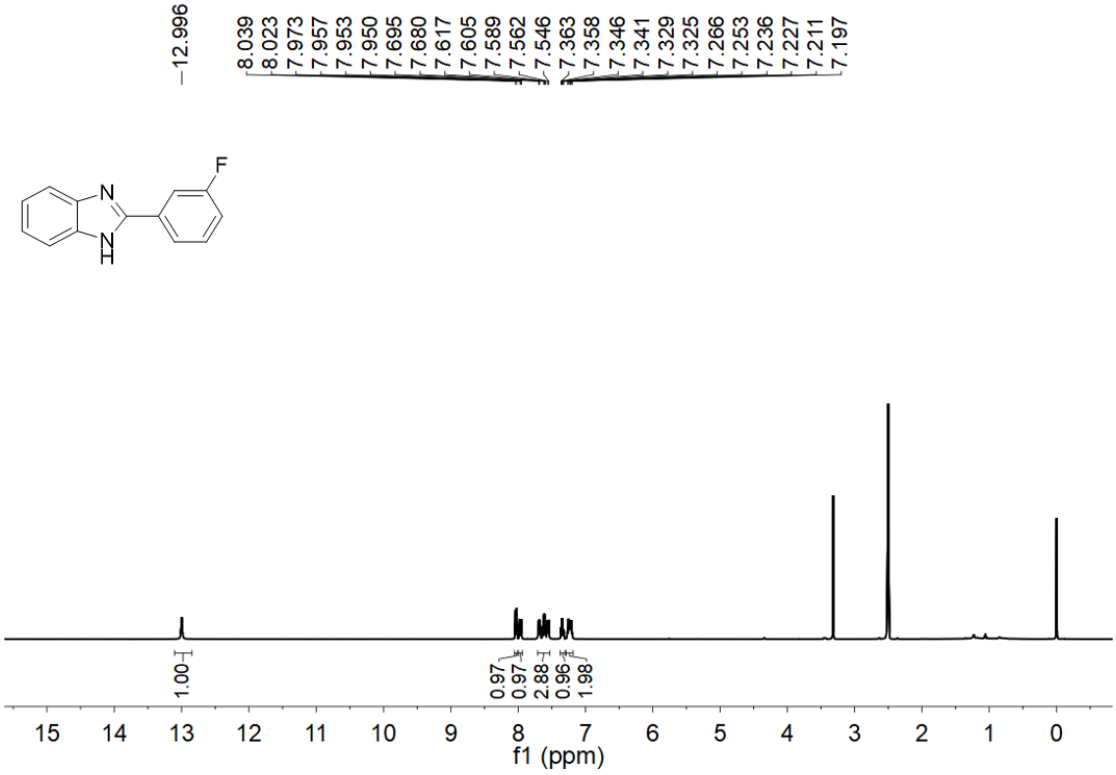

Fig. S22 ^{1}H NMR of 3e in DMSO.

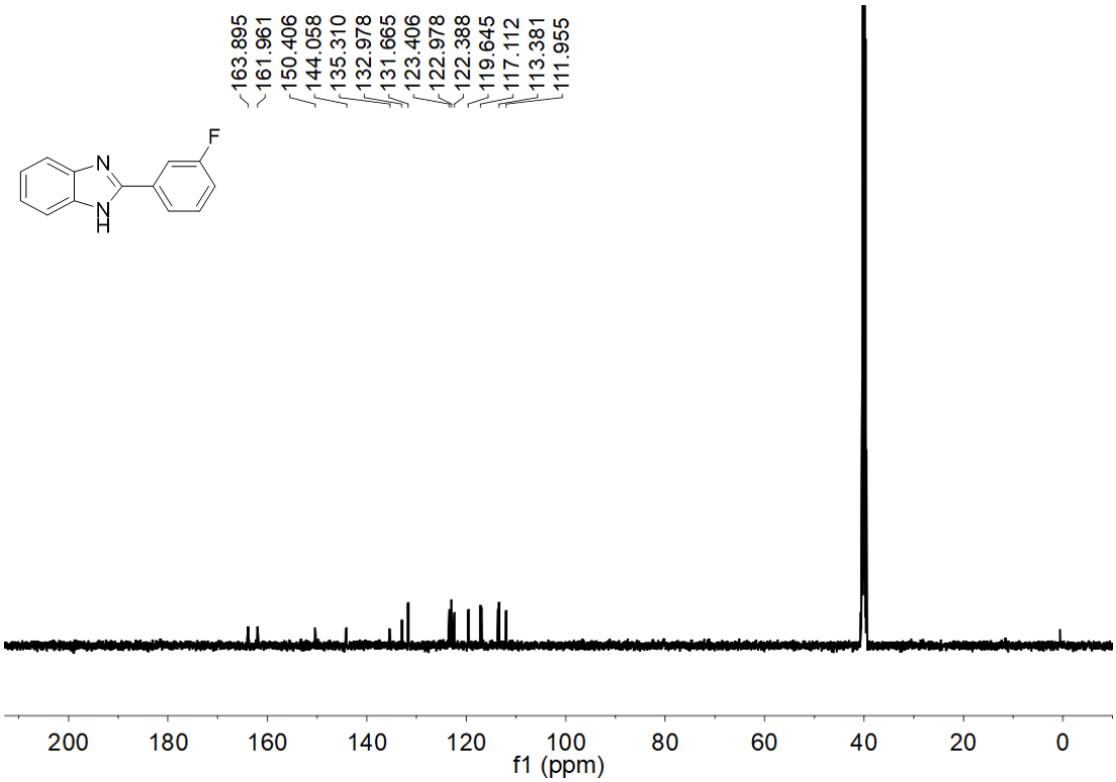

Fig. S23 ^{13}C NMR of 3e in DMSO.

^{1}H and ^{13}C Spectra of compound 3f (DMSO)

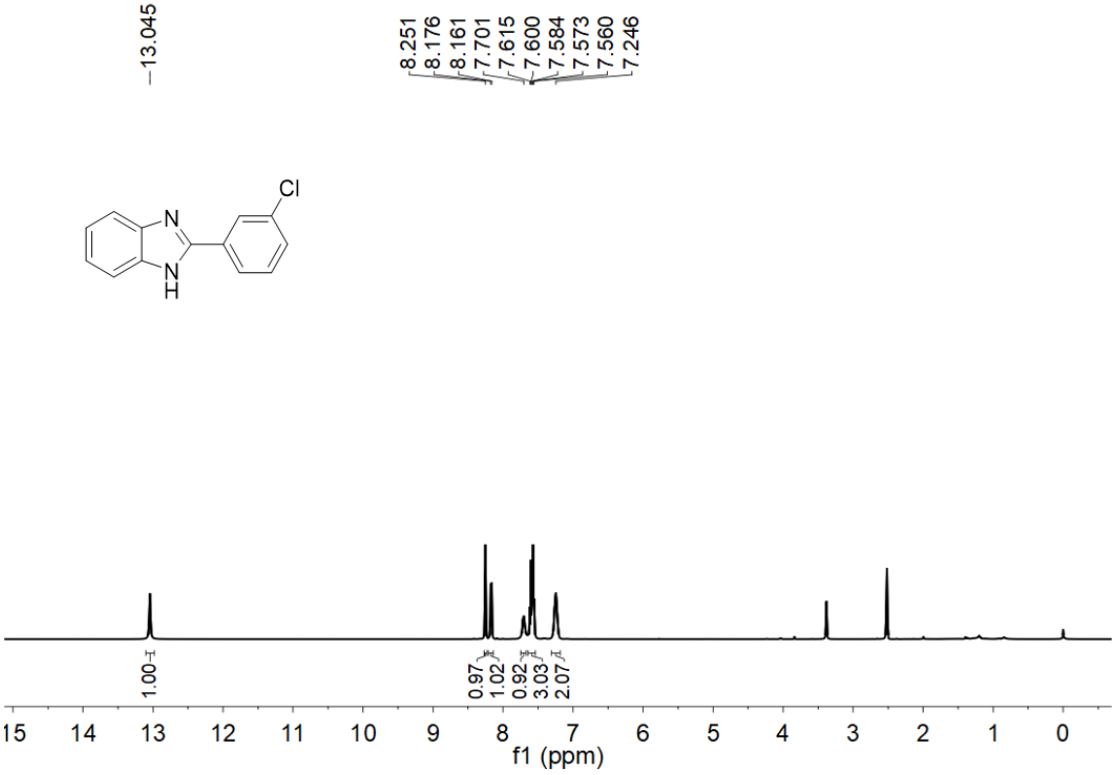

Fig. S24 ^{1}H NMR of 3f in DMSO.

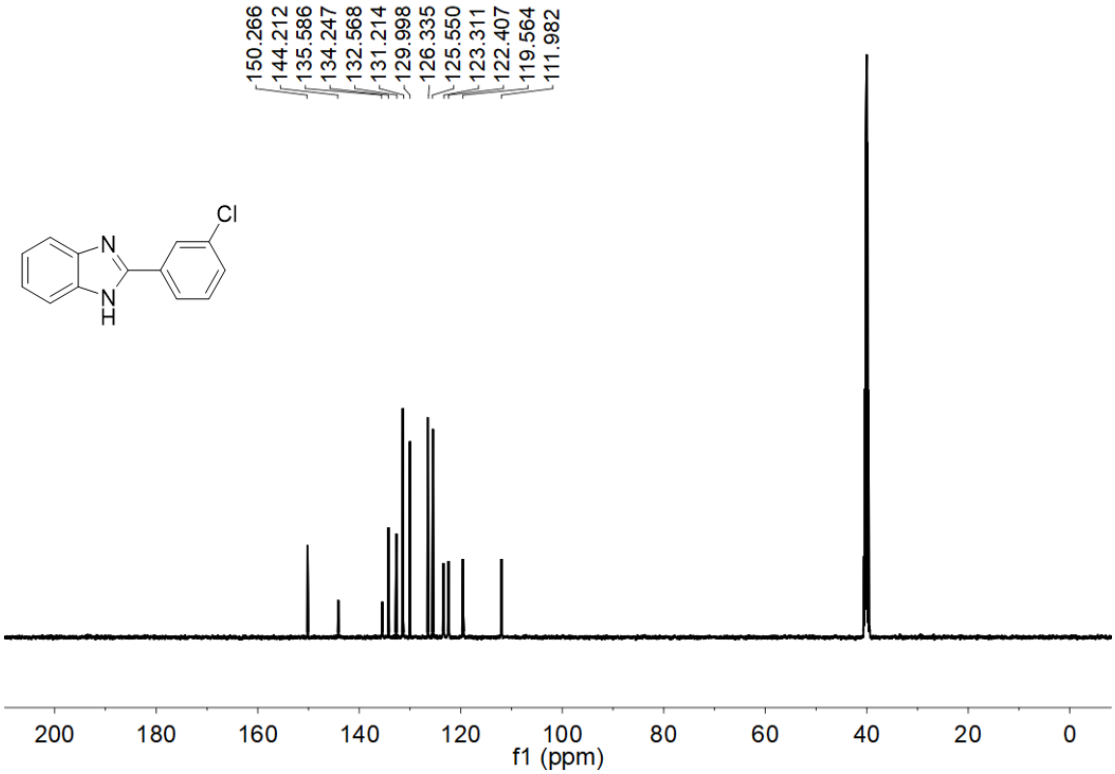

Fig. S25 ^{13}C NMR of 3f in DMSO.

^{1}H and ^{13}C Spectra of compound 3g (DMSO)

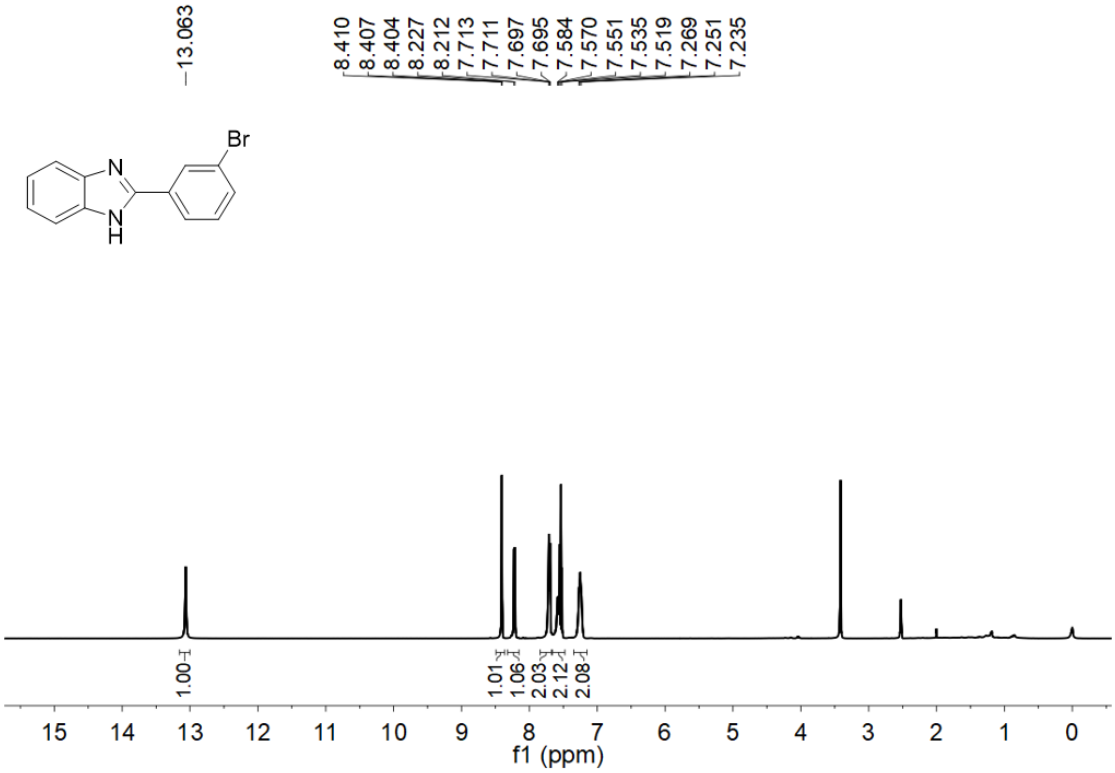

Fig. S26 ^{1}H NMR of 3g in DMSO.

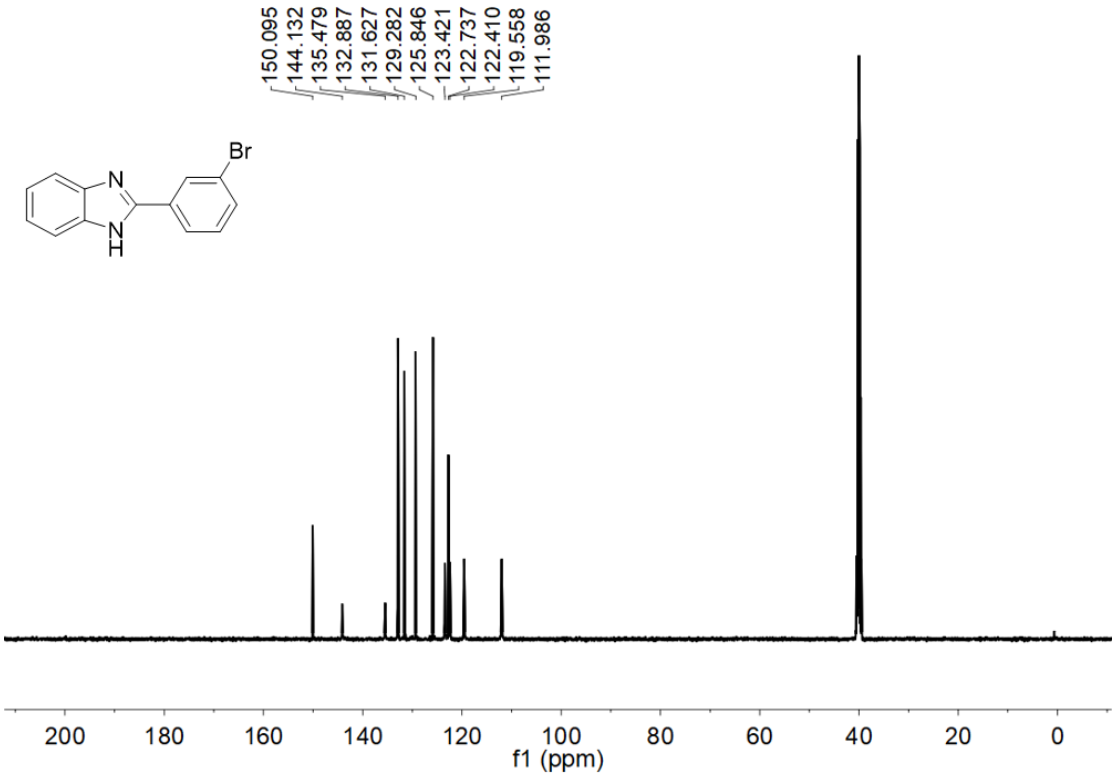

Fig. S27 ^{13}C NMR of 3g in DMSO.

^{1}H and ^{13}C Spectra of compound 3h (DMSO)

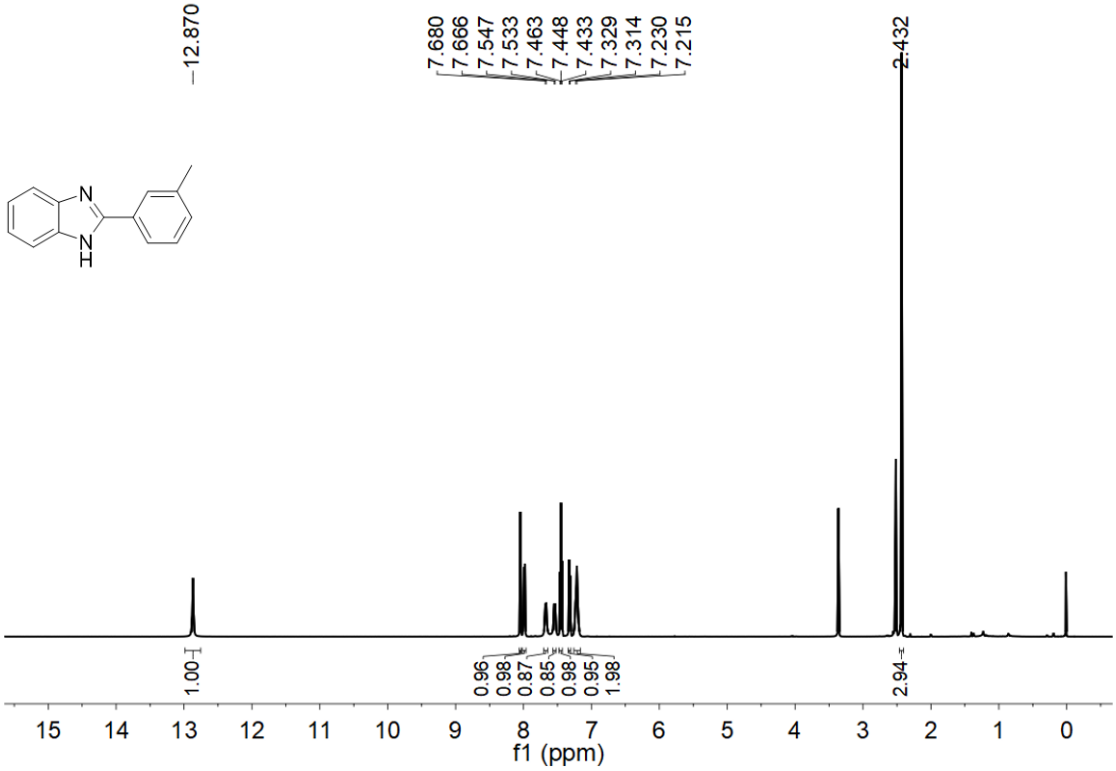

Fig. S28 ^{1}H NMR of 3h in DMSO.

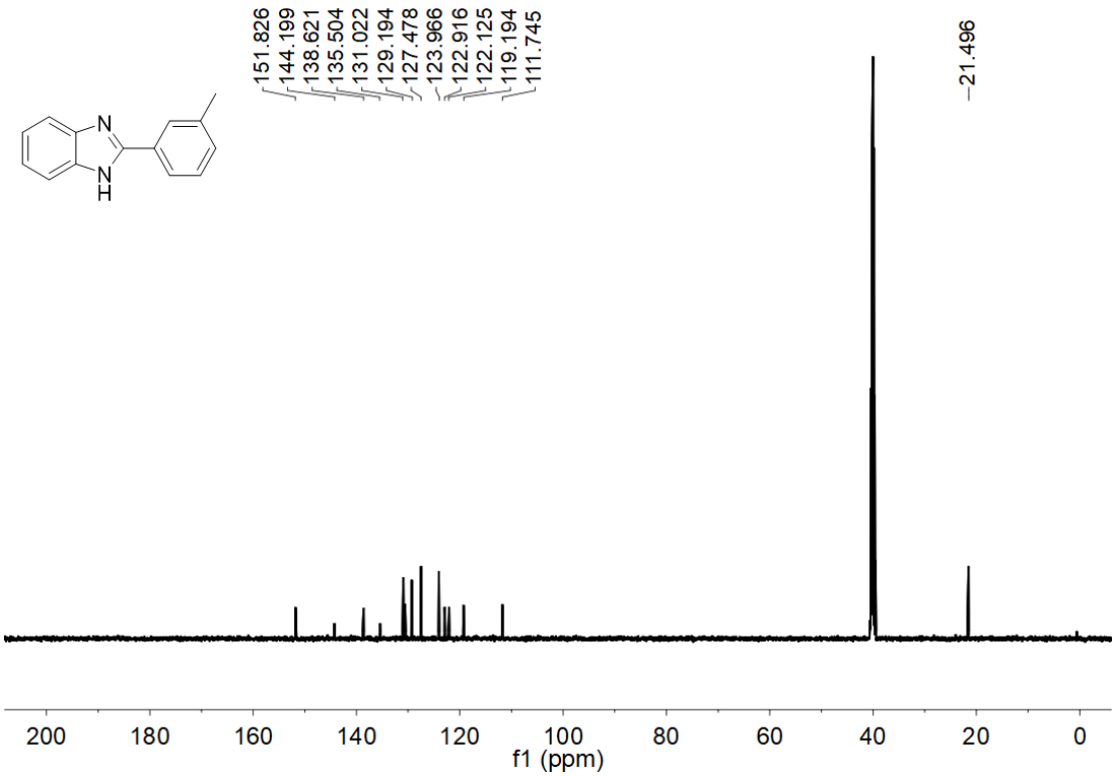

Fig. S29 ^{13}C NMR of 3h in DMSO.

^{1}H and ^{13}C Spectra of compound 3i (DMSO)

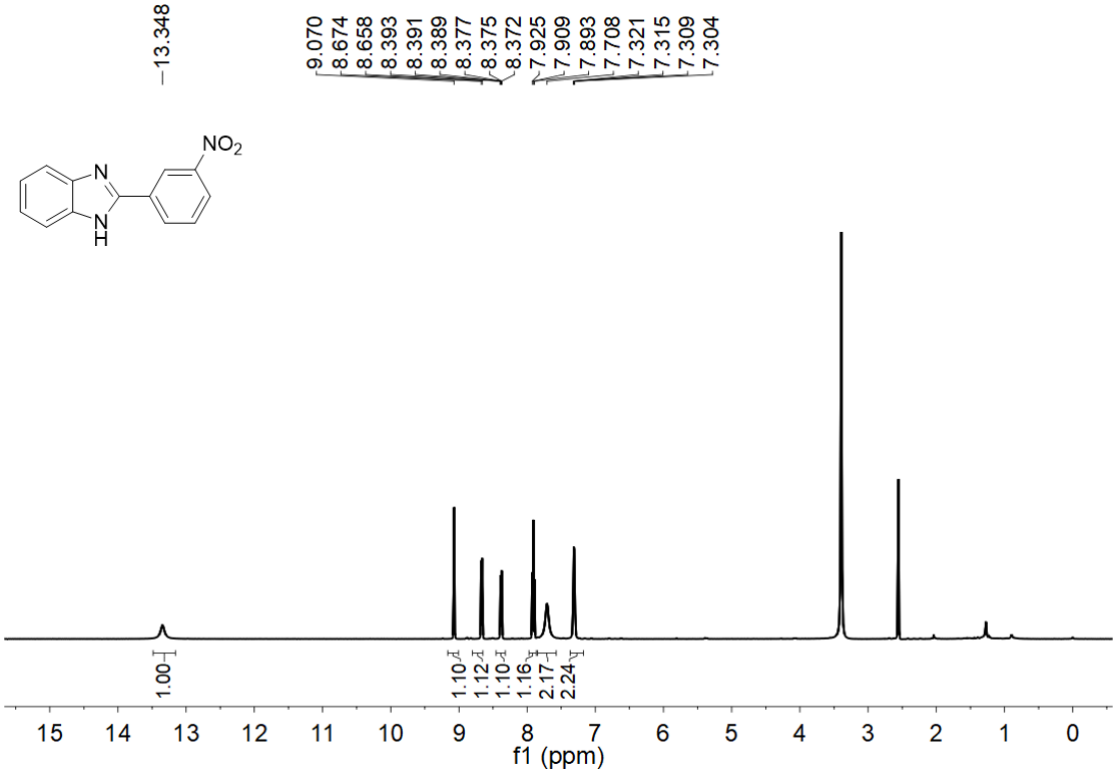

Fig. S30 ^{1}H NMR of 3i in DMSO.

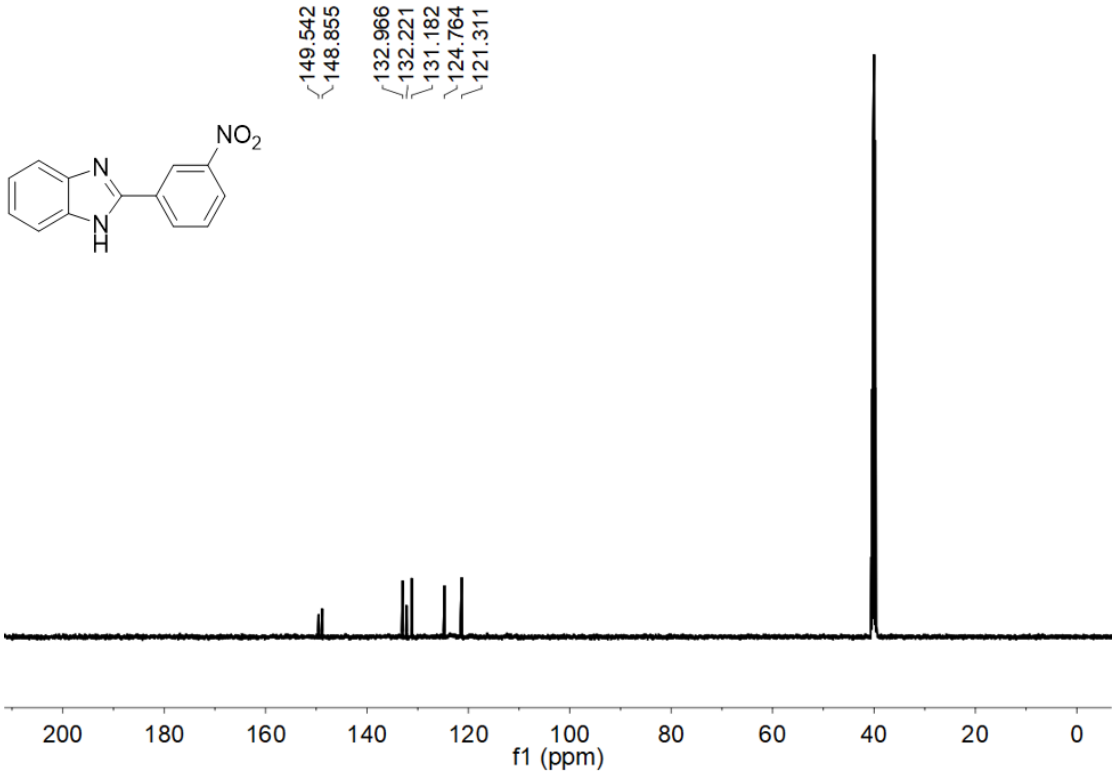

Fig. S31 ^{13}C NMR of 3i in DMSO.

^{1}H and ^{13}C Spectra of compound 3j (DMSO)

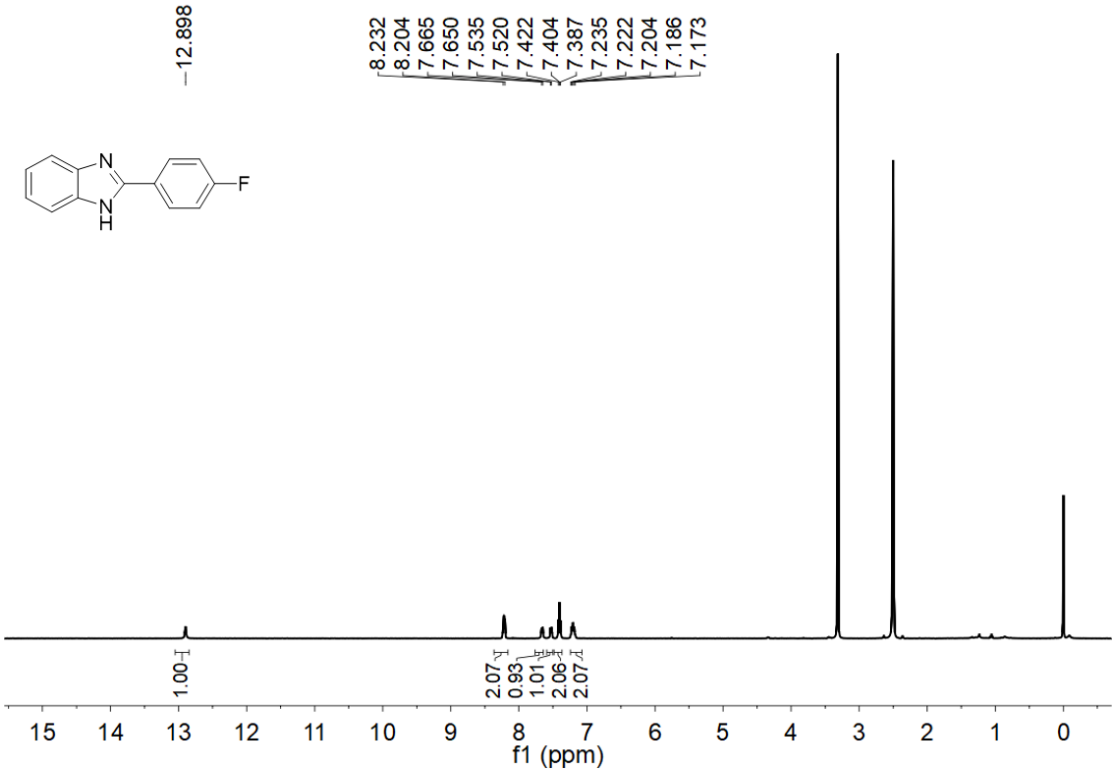

Fig. S32 ^{1}H NMR of 3j in DMSO.

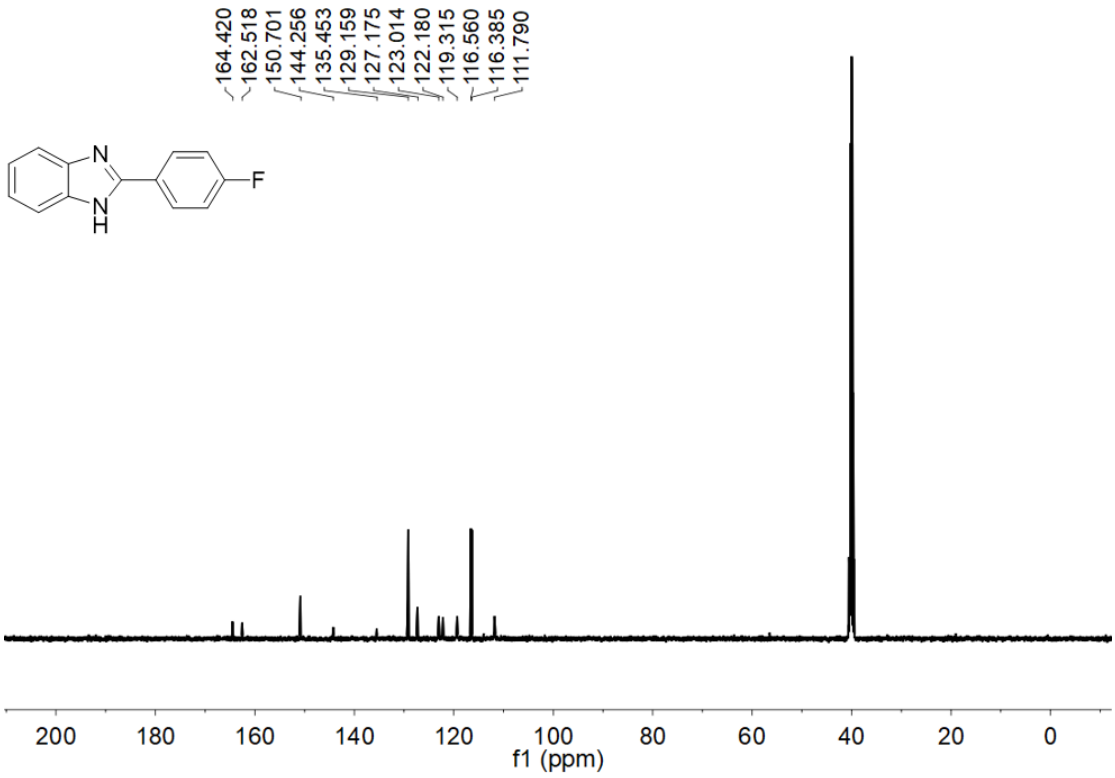

Fig. S33 ^{13}C NMR of 3j in DMSO.

^{1}H and ^{13}C Spectra of compound 3k (DMSO)

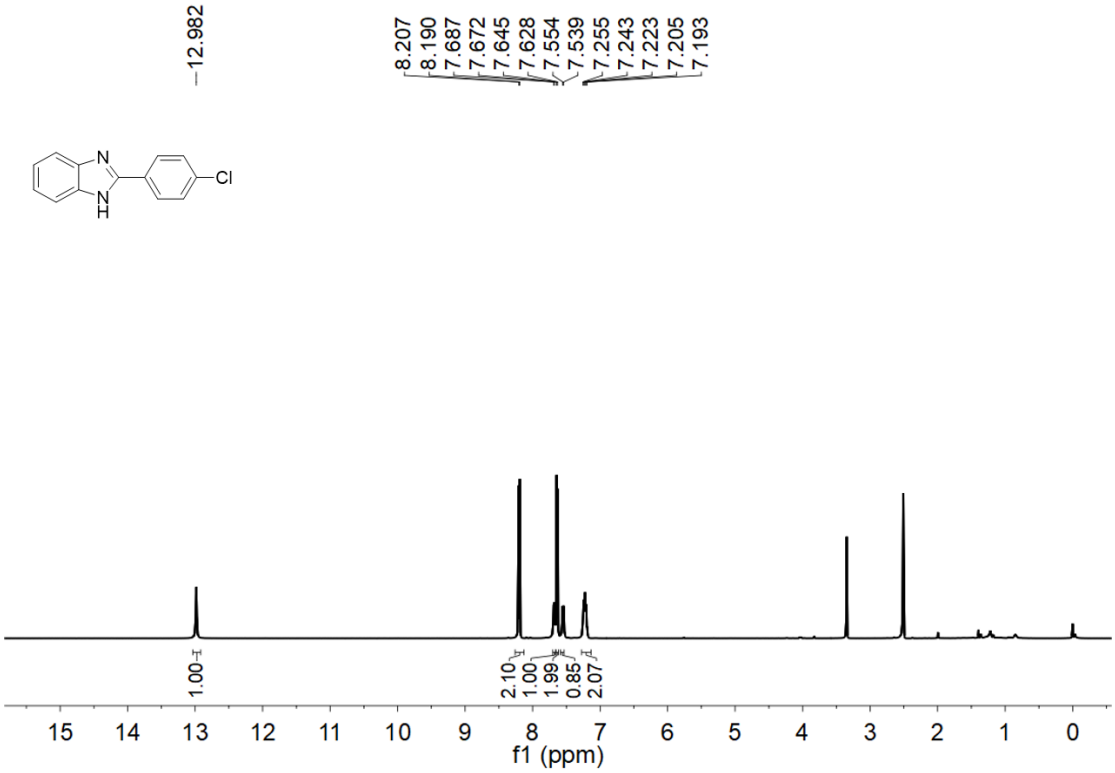

Fig. S34 ^{1}H NMR of 3k in DMSO.

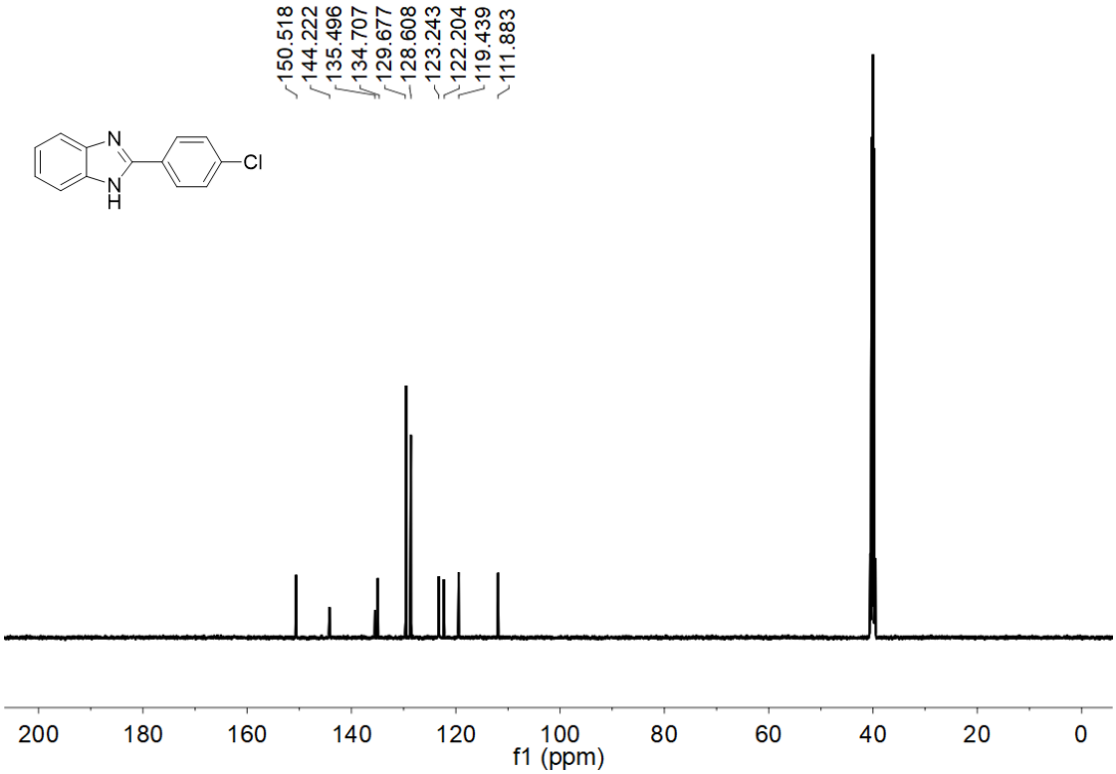

Fig. S35 ^{13}C NMR of 3k in DMSO.

^{1}H and ^{13}C Spectra of compound 3l (DMSO)

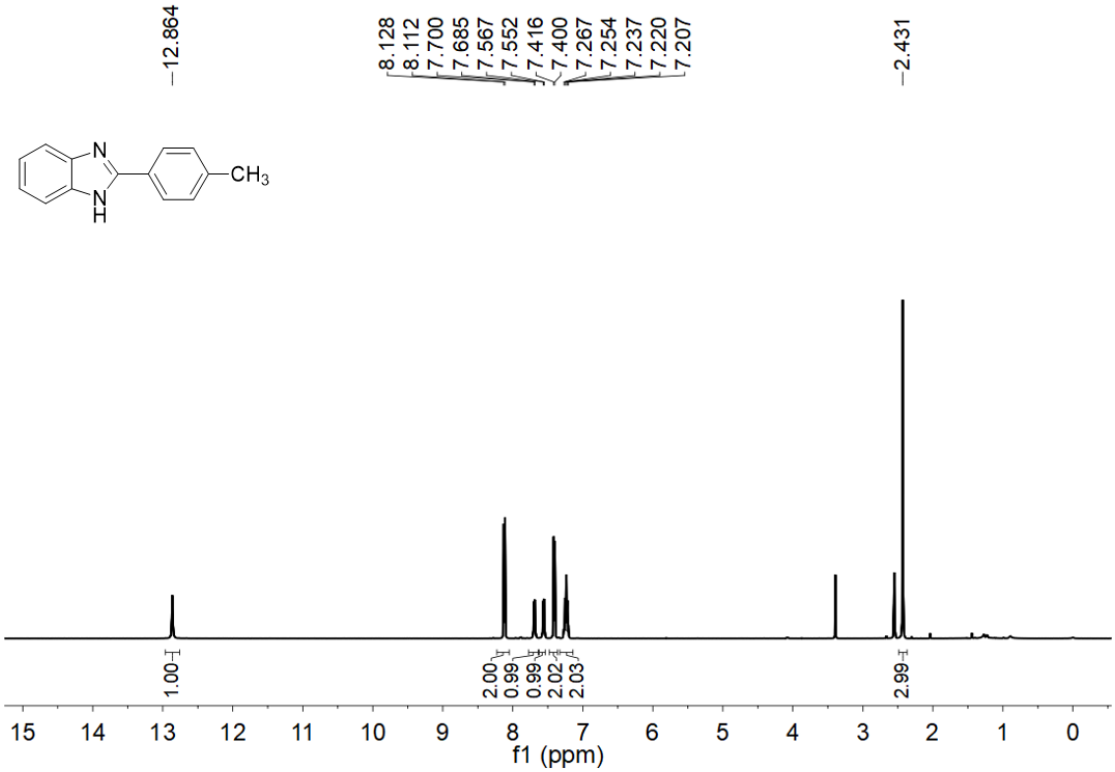

Fig. S36 ^{1}H NMR of 3l in DMSO.

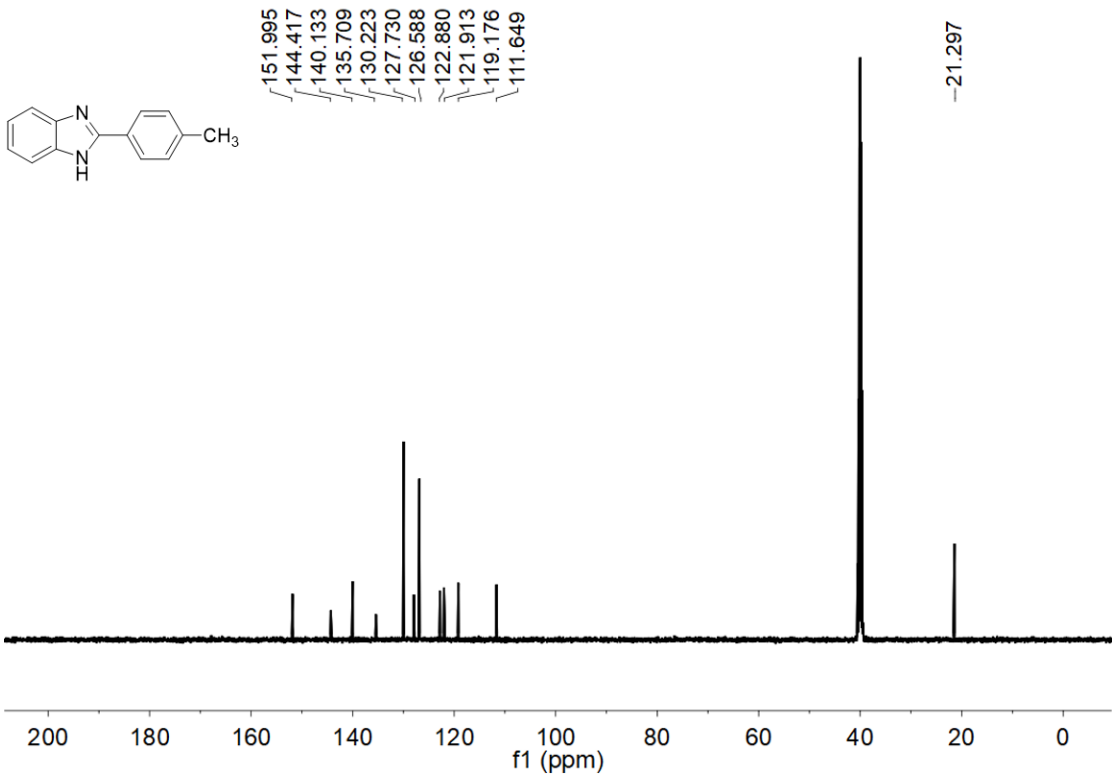

Fig. S37 ^{13}C NMR of 3l in DMSO.

^{1}H and ^{13}C Spectra of compound 3m (DMSO)

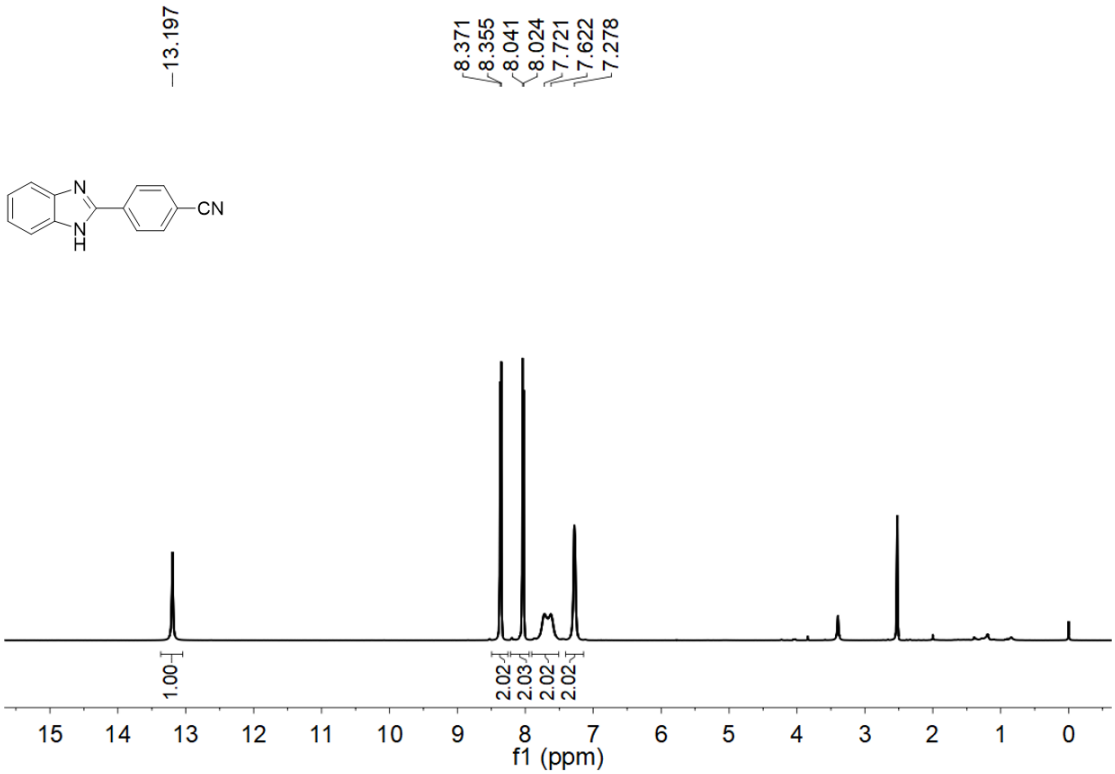

Fig. S38 ^{1}H NMR of 3m in DMSO.

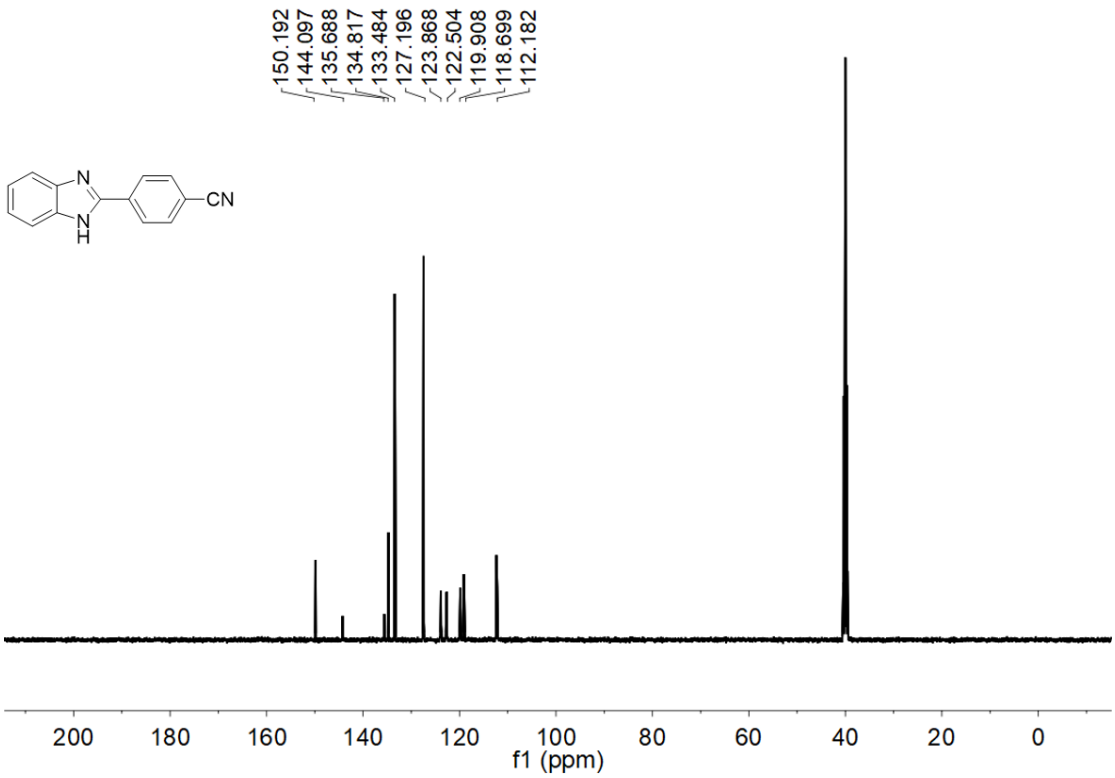

Fig. S39 ^{13}C NMR of 3m in DMSO.

^{1}H and ^{13}C Spectra of compound 3n (DMSO)

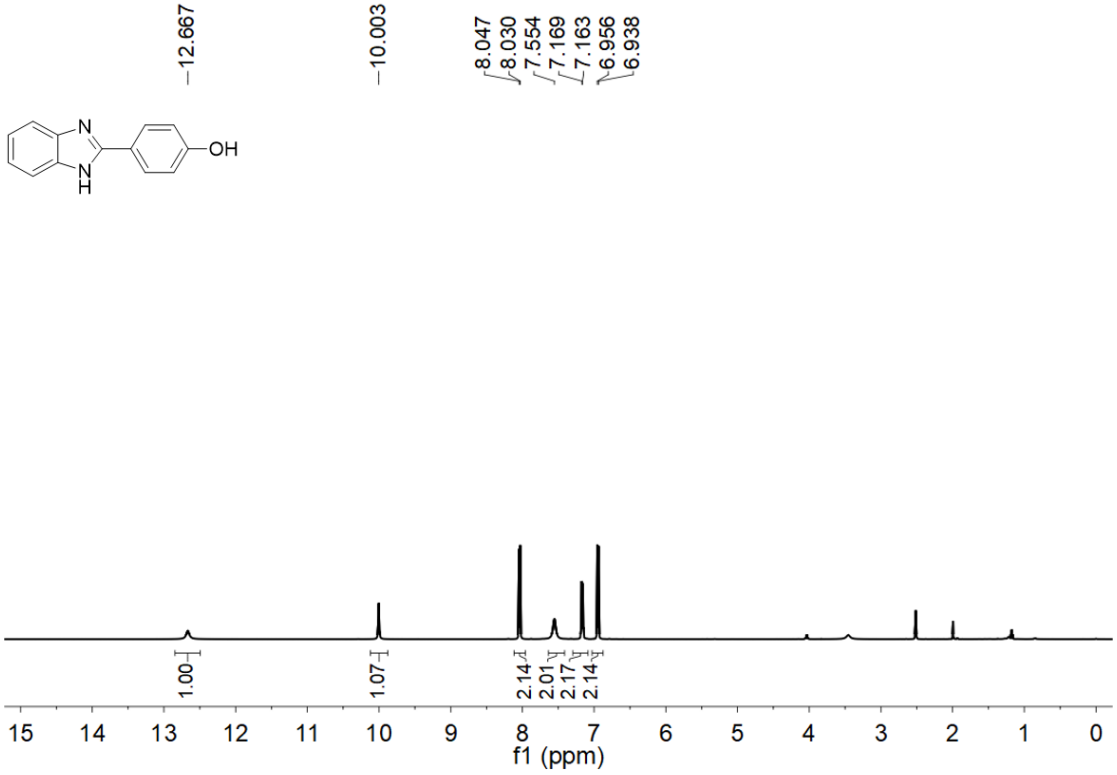

Fig. S40 ^{1}H NMR of 3n in DMSO.

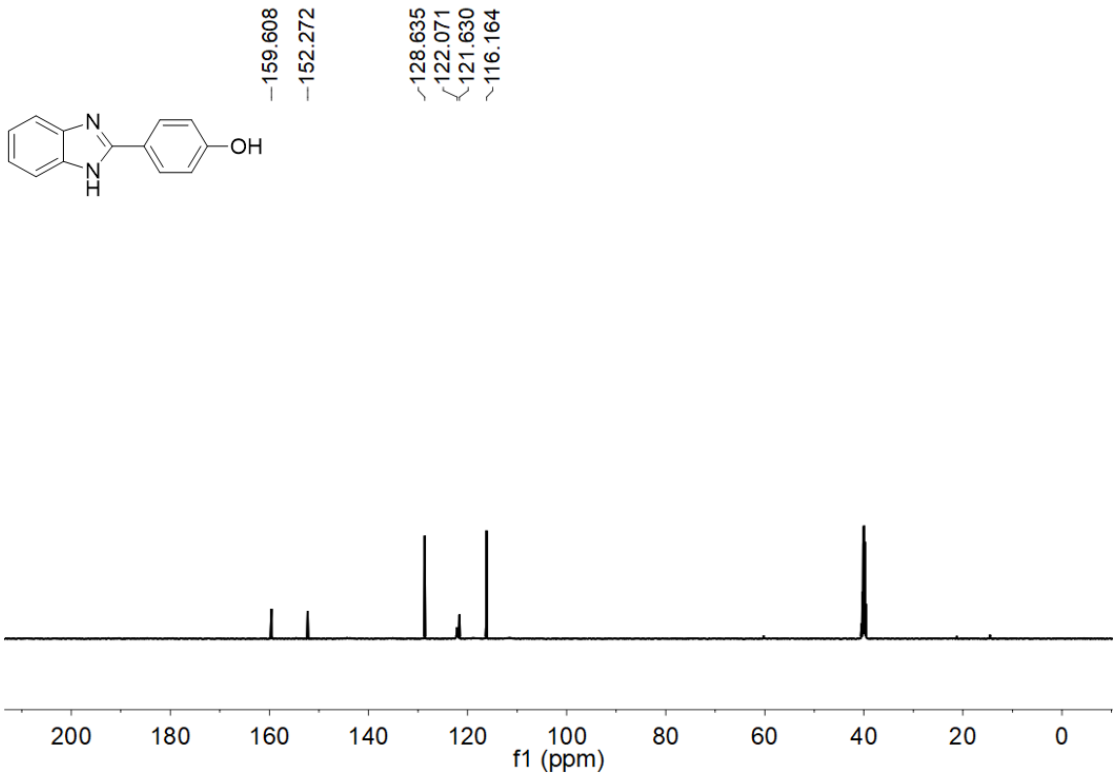

Fig. S41 ^{13}C NMR of 3n in DMSO.

^{1}H and ^{13}C Spectra of compound 3o (DMSO)

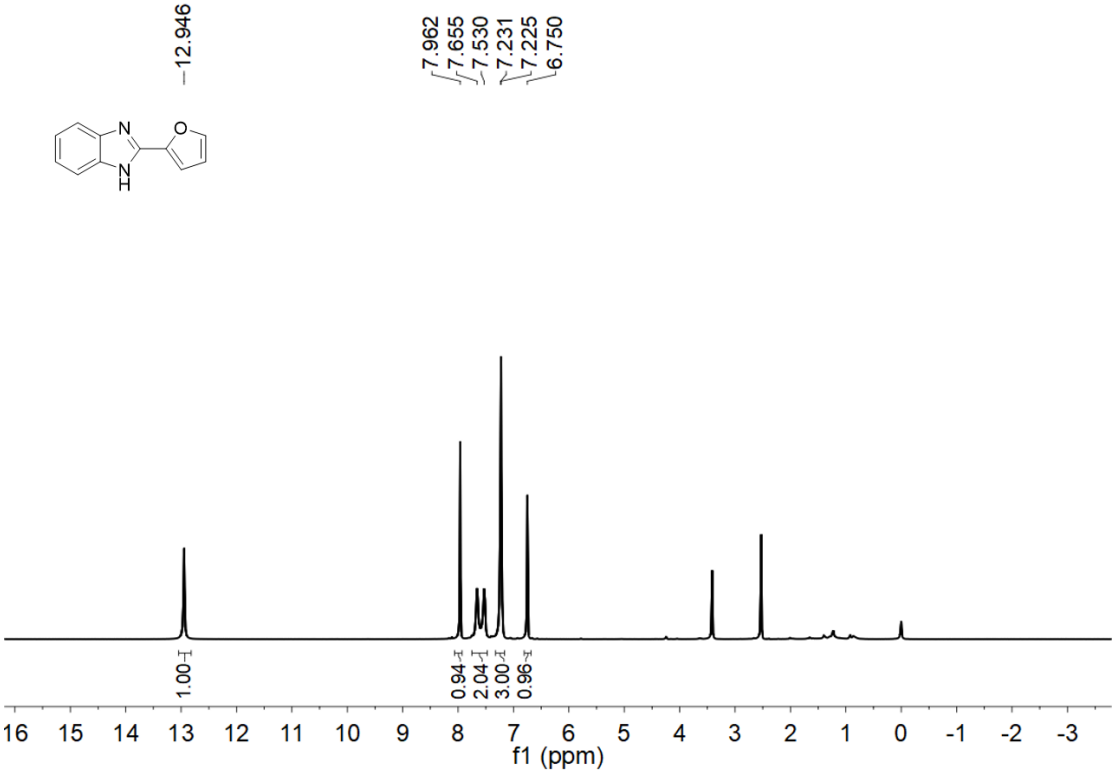

Fig. S42 ^{1}H NMR of 3o in DMSO.

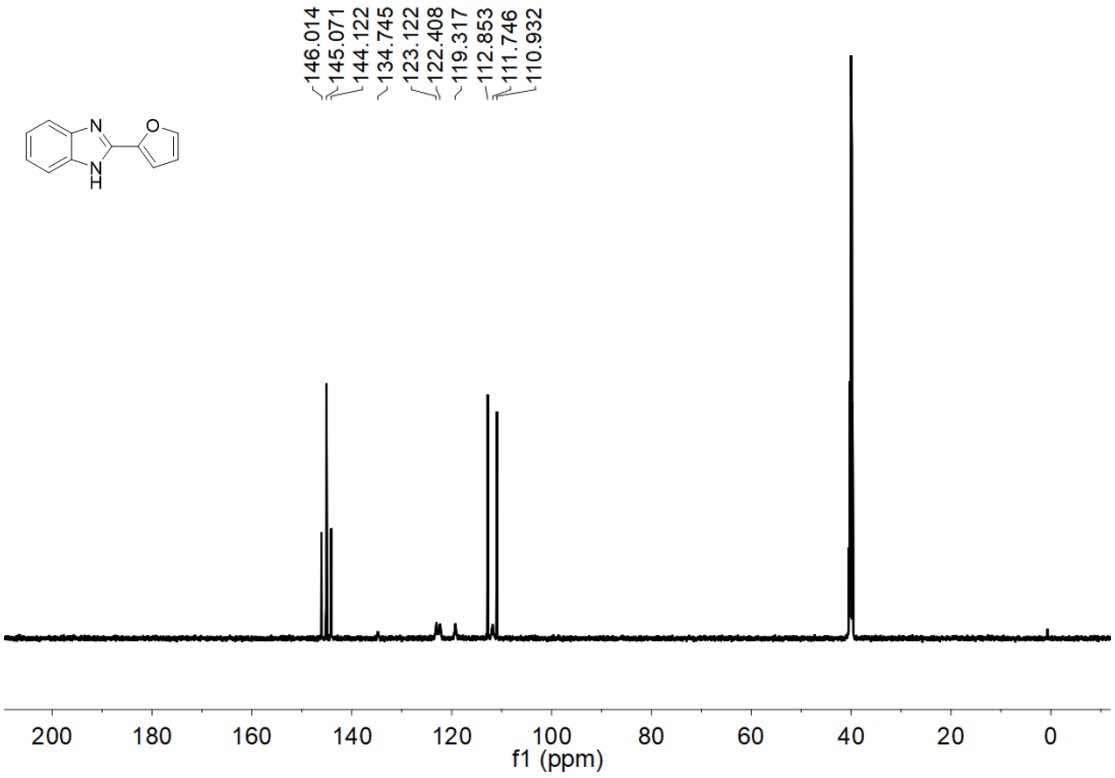

Fig. S43 ^{13}C NMR of 3o in DMSO.

^{1}H and ^{13}C Spectra of compound 3p (DMSO)

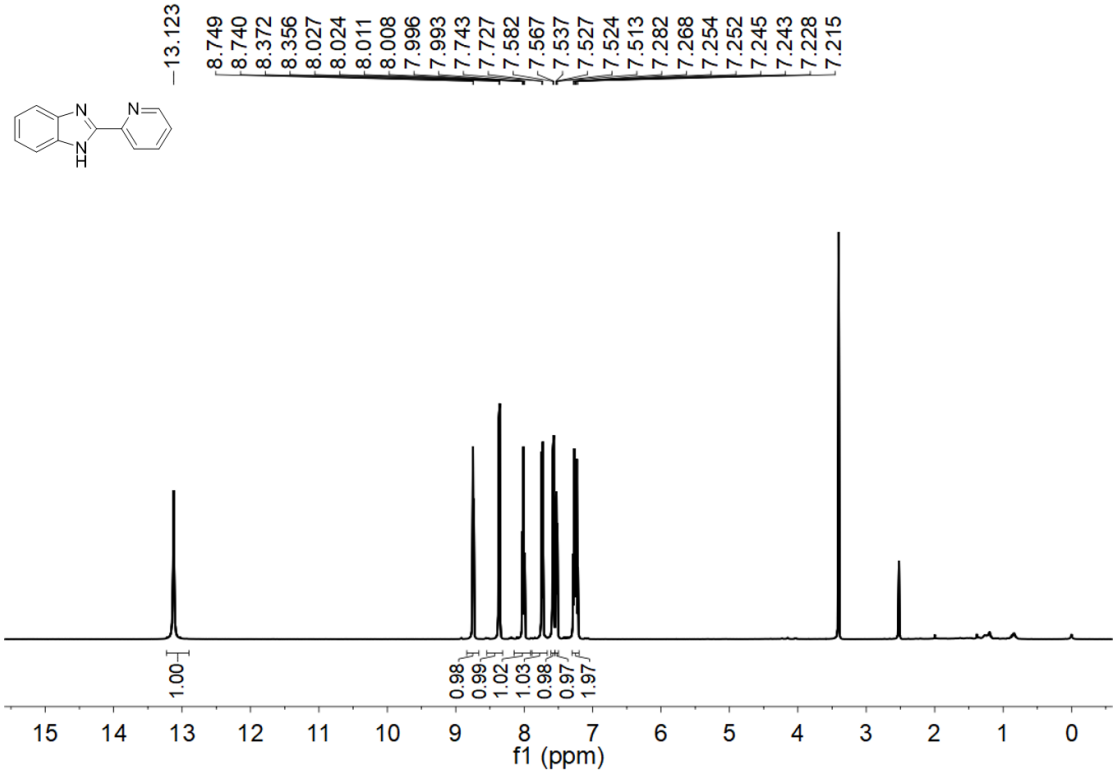

Fig. S44 ^{1}H NMR of 3p in DMSO.

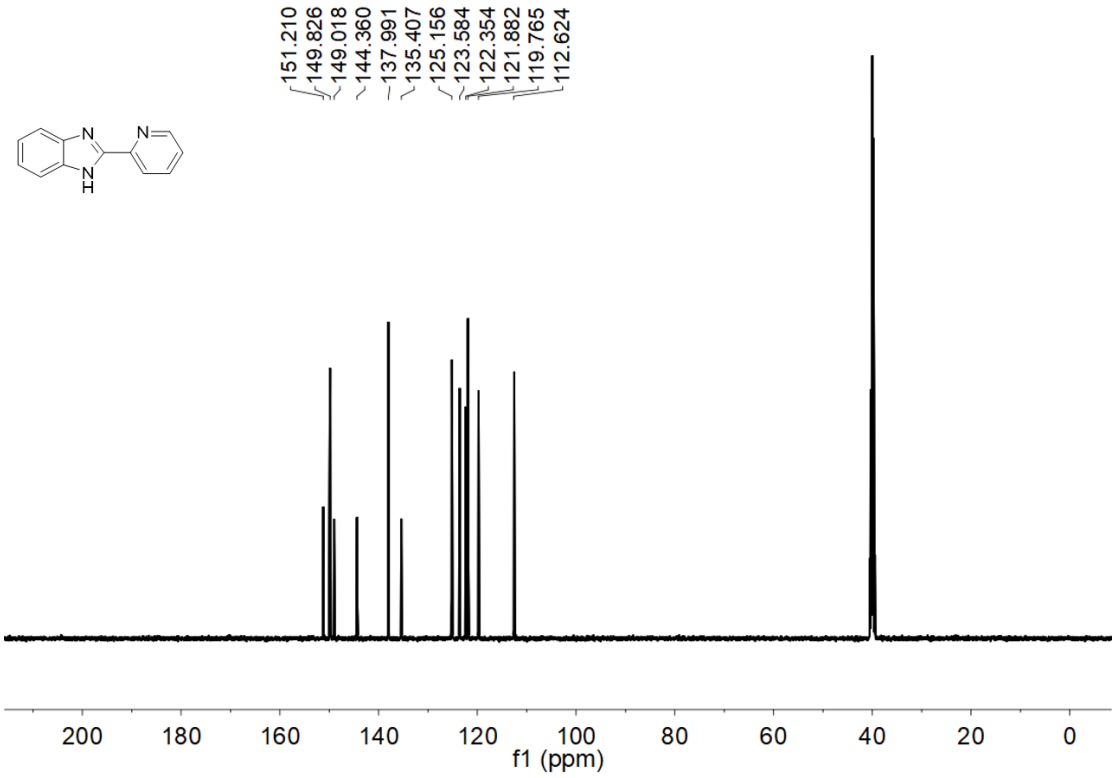

Fig. S45 ^{13}C NMR of 3p in DMSO.

^{1}H and ^{13}C Spectra of compound 3q (DMSO)

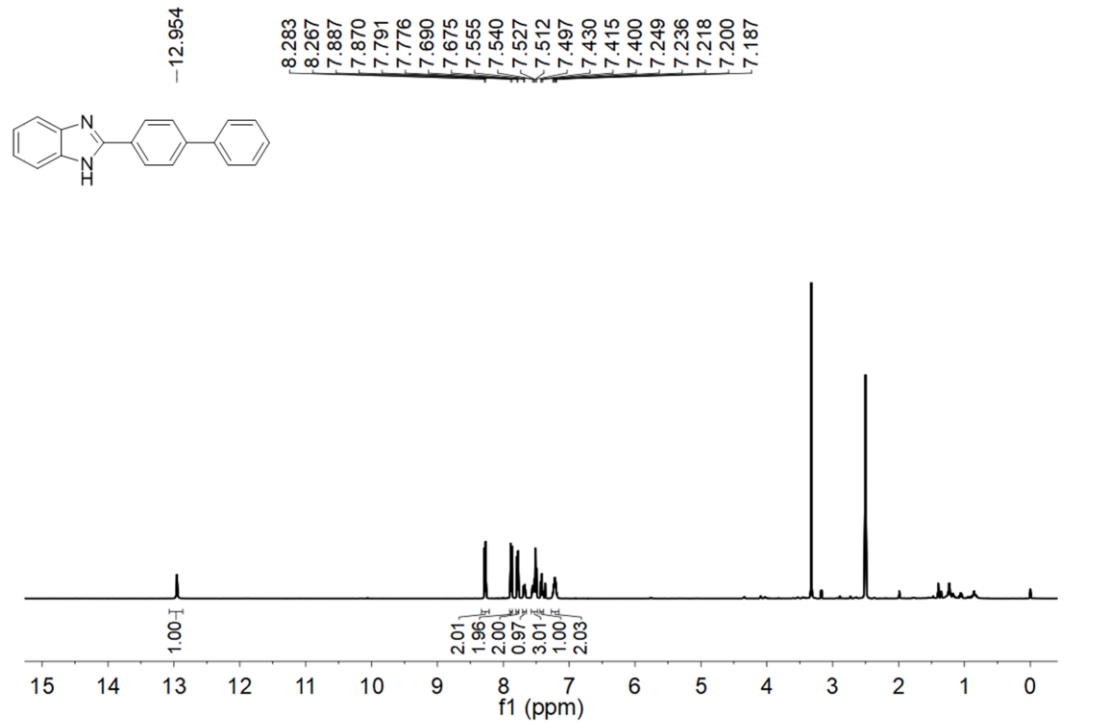

Fig. S46 ^{1}H NMR of 3q in DMSO.

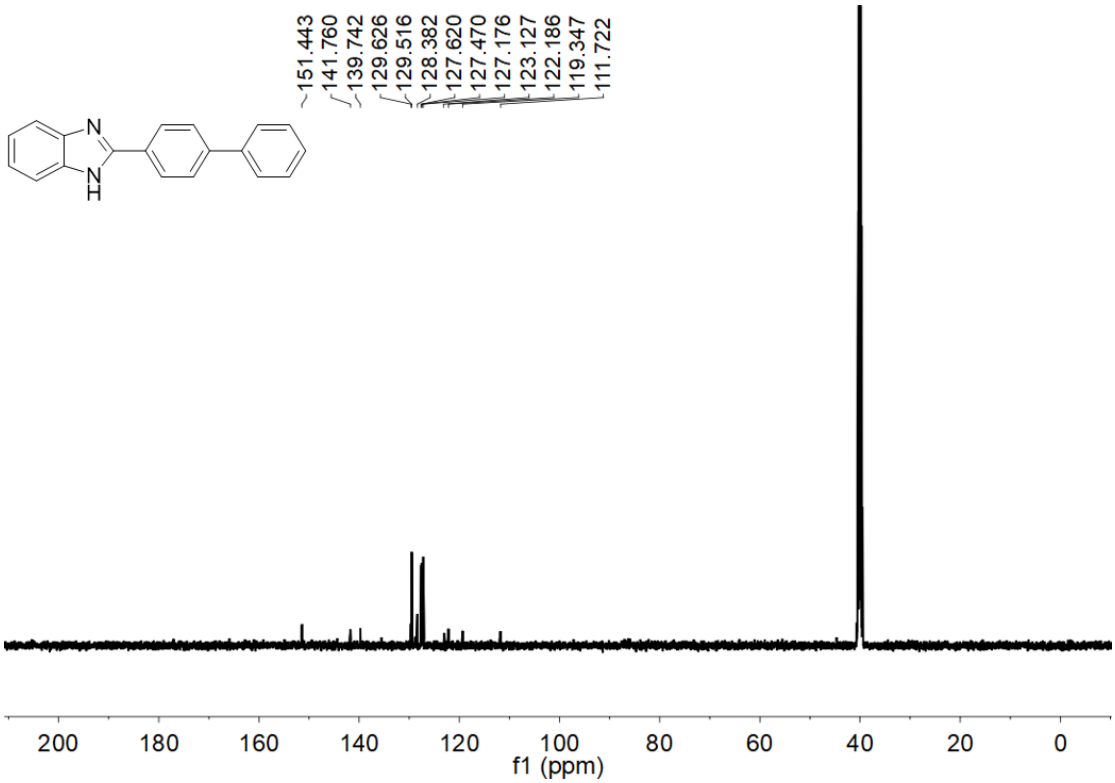

Fig. S47 ^{13}C NMR of 3q in DMSO.

^{1}H and ^{13}C Spectra of compound 3r (DMSO)

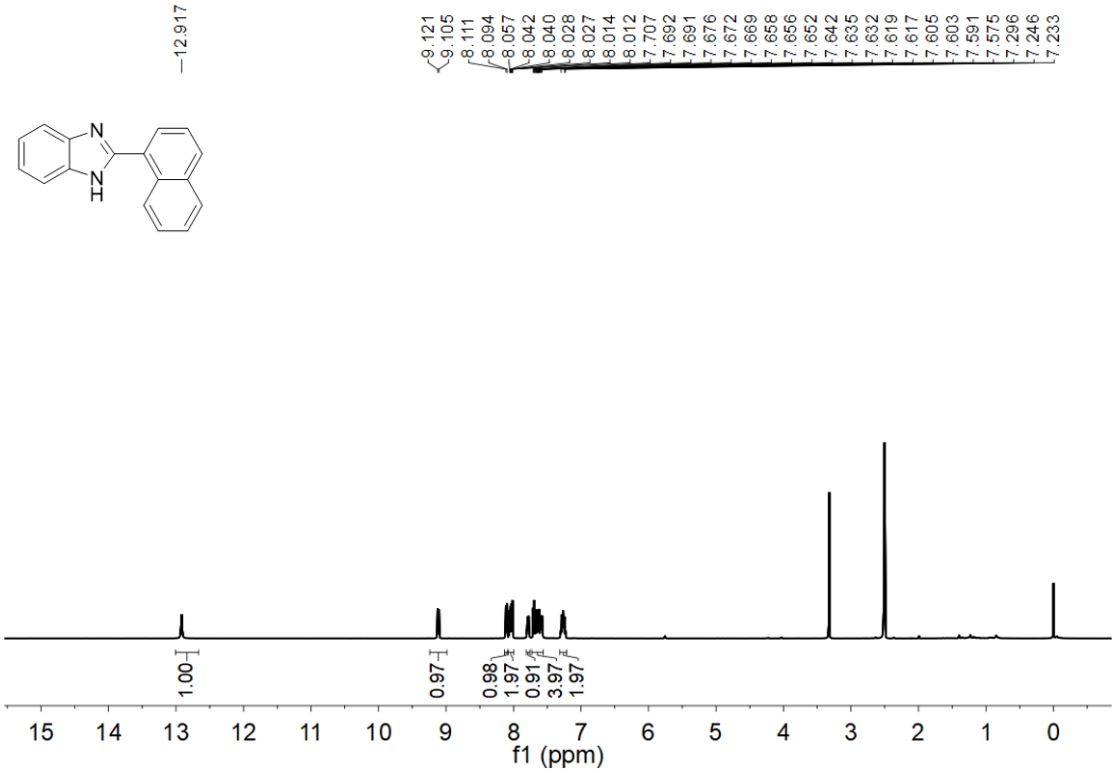

Fig. S48 ^{1}H NMR of 3r in DMSO.

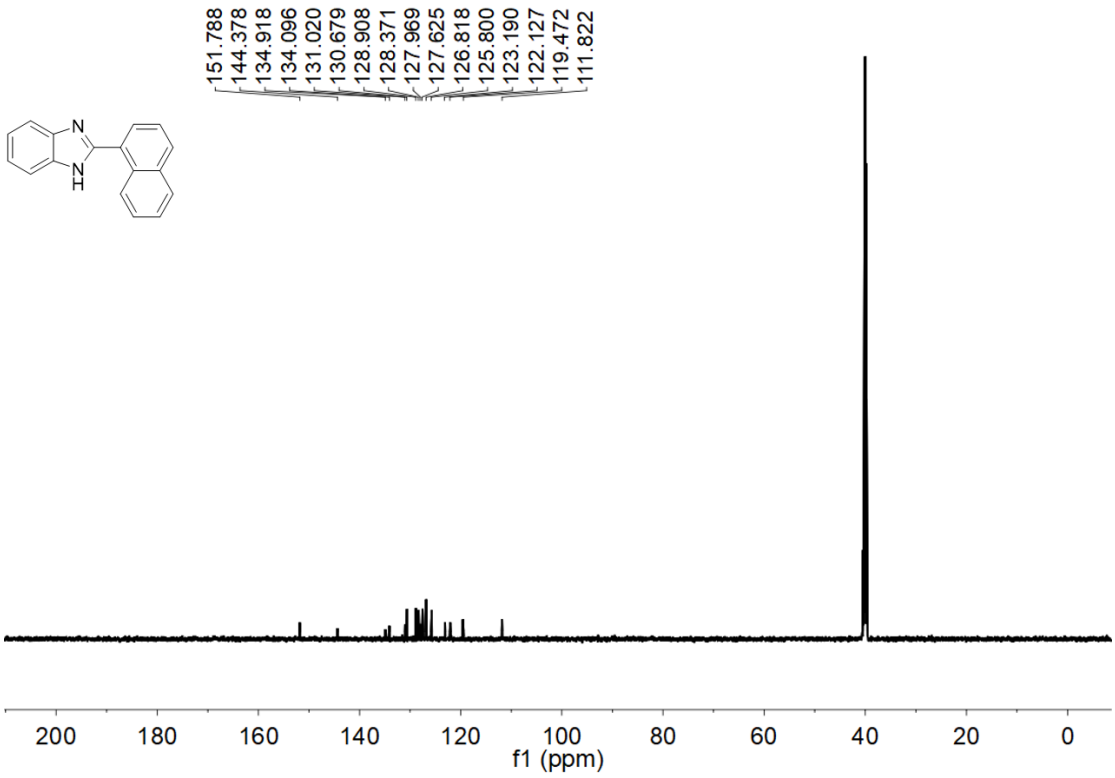

Fig. S49 ^{13}C NMR of 3r in DMSO.

^{1}H and ^{13}C Spectra of compound 3s (DMSO)

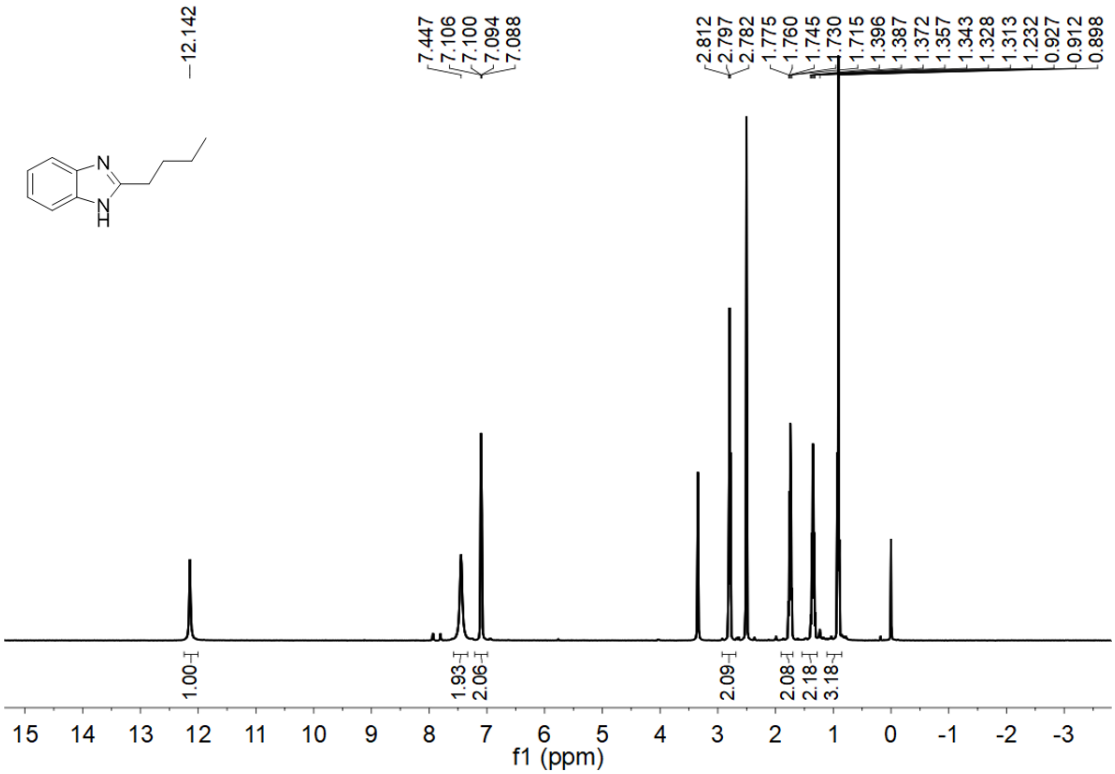

Fig. S50 ^{1}H NMR of 3s in DMSO.

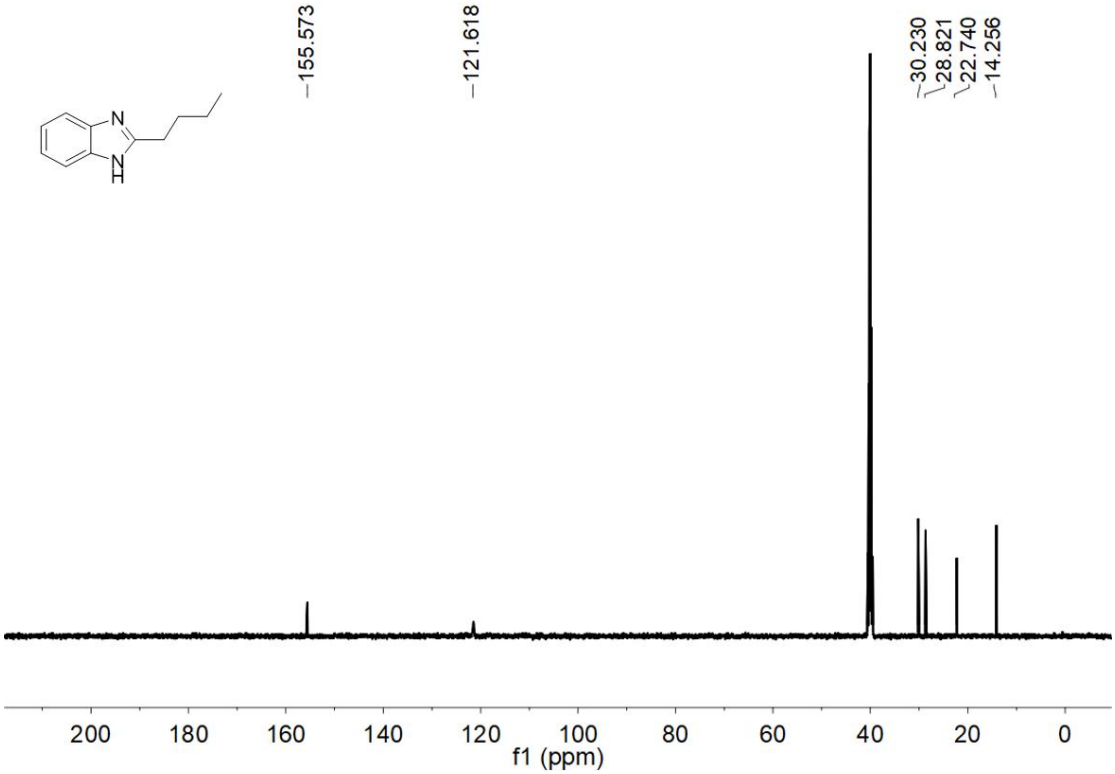

Fig. S51 ^{13}C NMR of 3s in DMSO.

^{1}H and ^{13}C Spectra of compound 3t (DMSO)

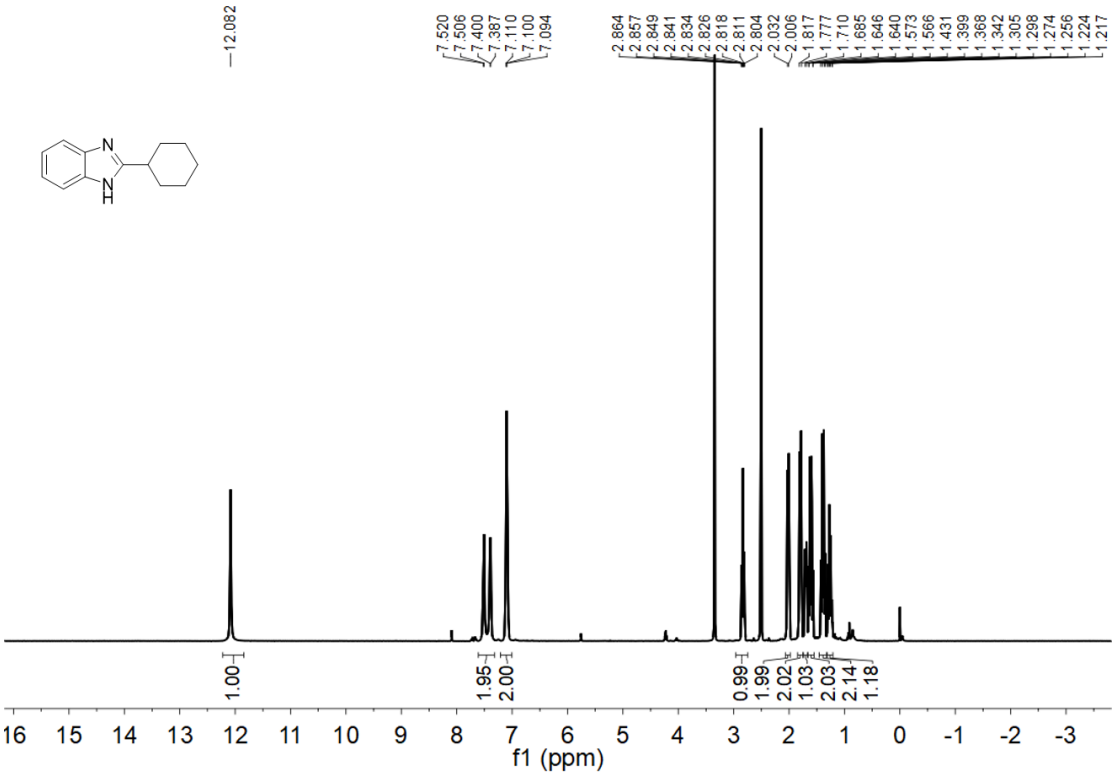

Fig. S52 ^{1}H NMR of 3t in DMSO.

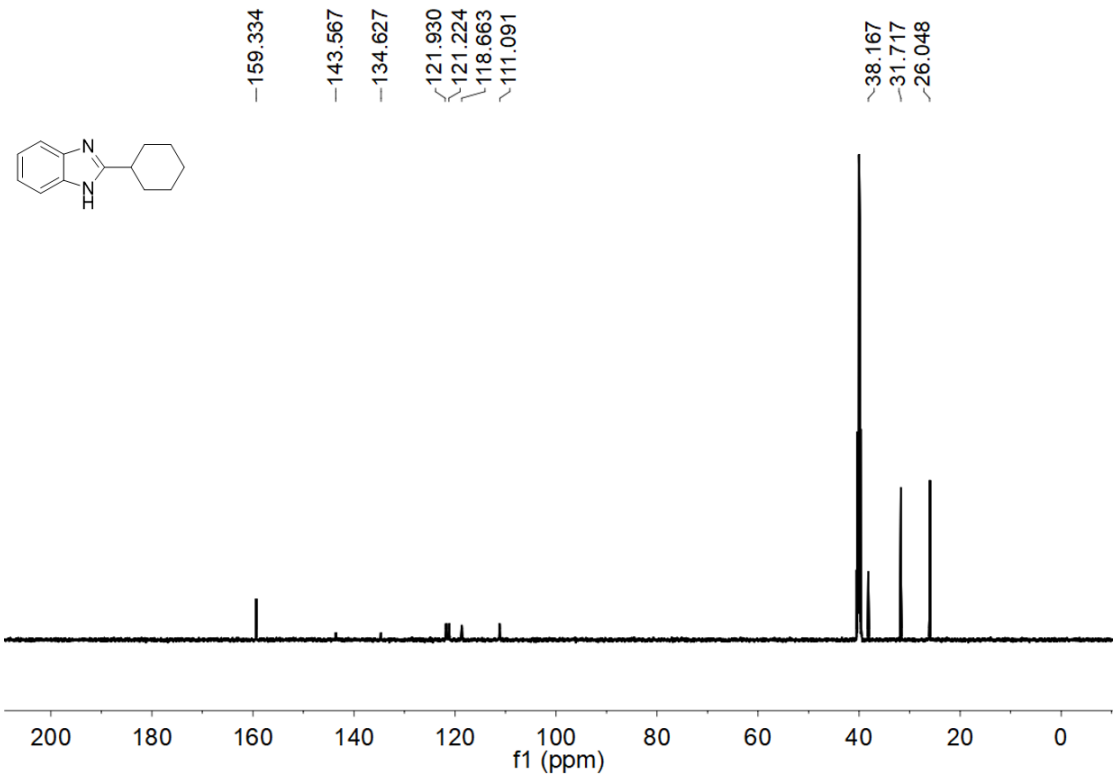

Fig. S53 ^{13}C NMR of 3t in DMSO.

^{1}H and ^{13}C Spectra of compound 3u (DMSO)

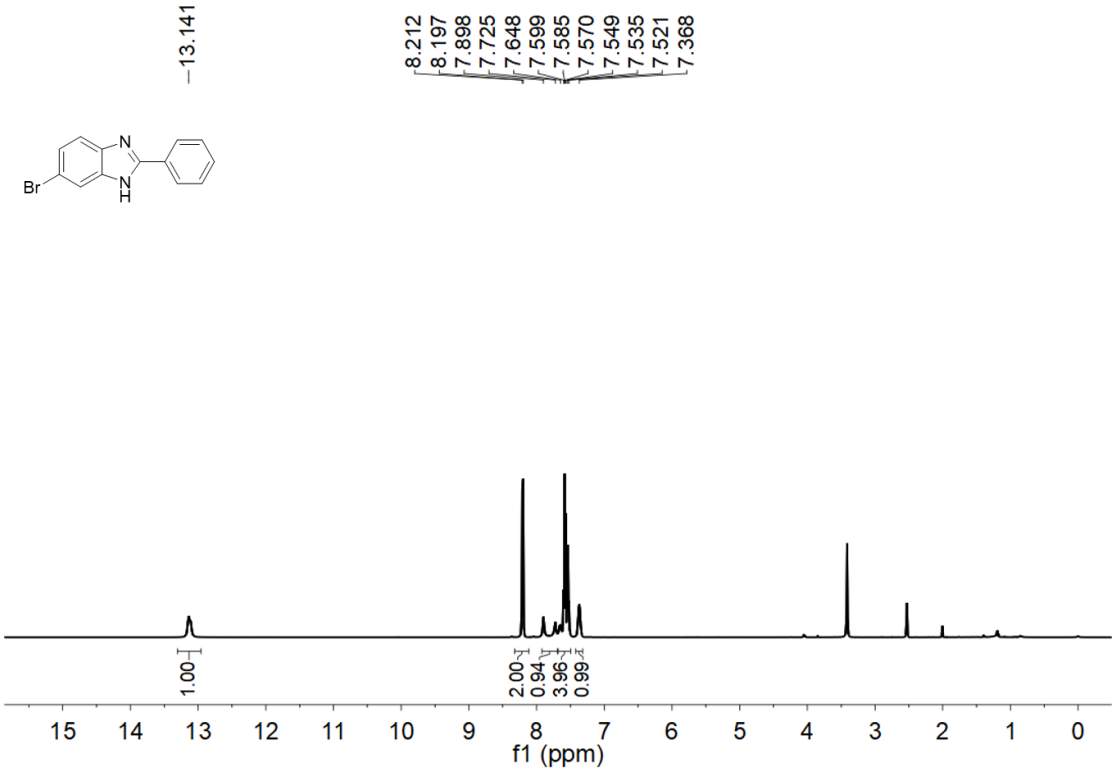

Fig. S54 ^{1}H NMR of 3u in DMSO.

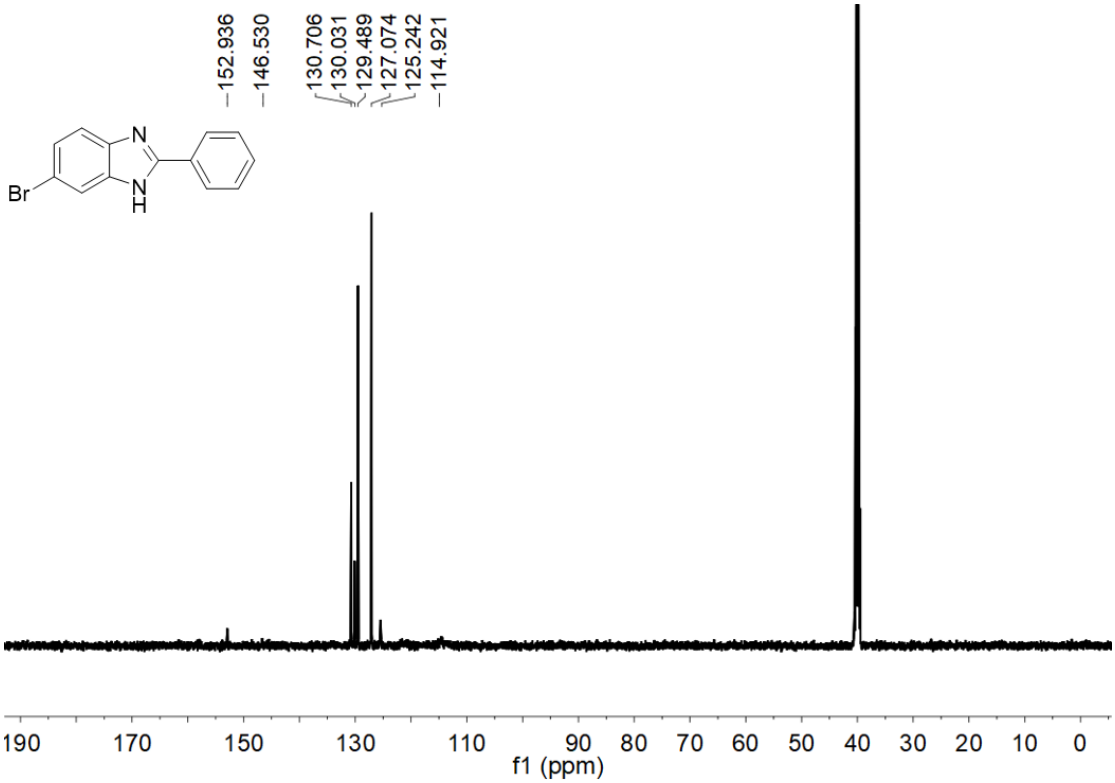

Fig. S55 ^{13}C NMR of 3u in DMSO.

^{1}H and ^{13}C Spectra of compound 3v (DMSO)

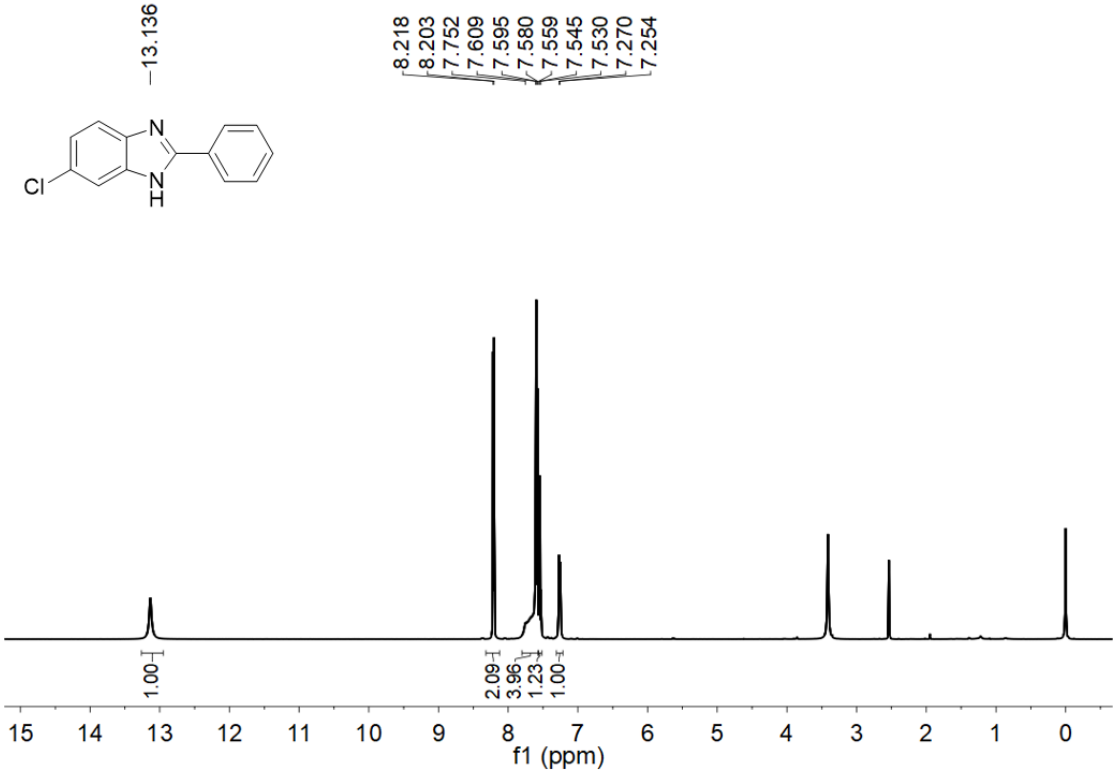

Fig. S56 ^{1}H NMR of 3v in DMSO.

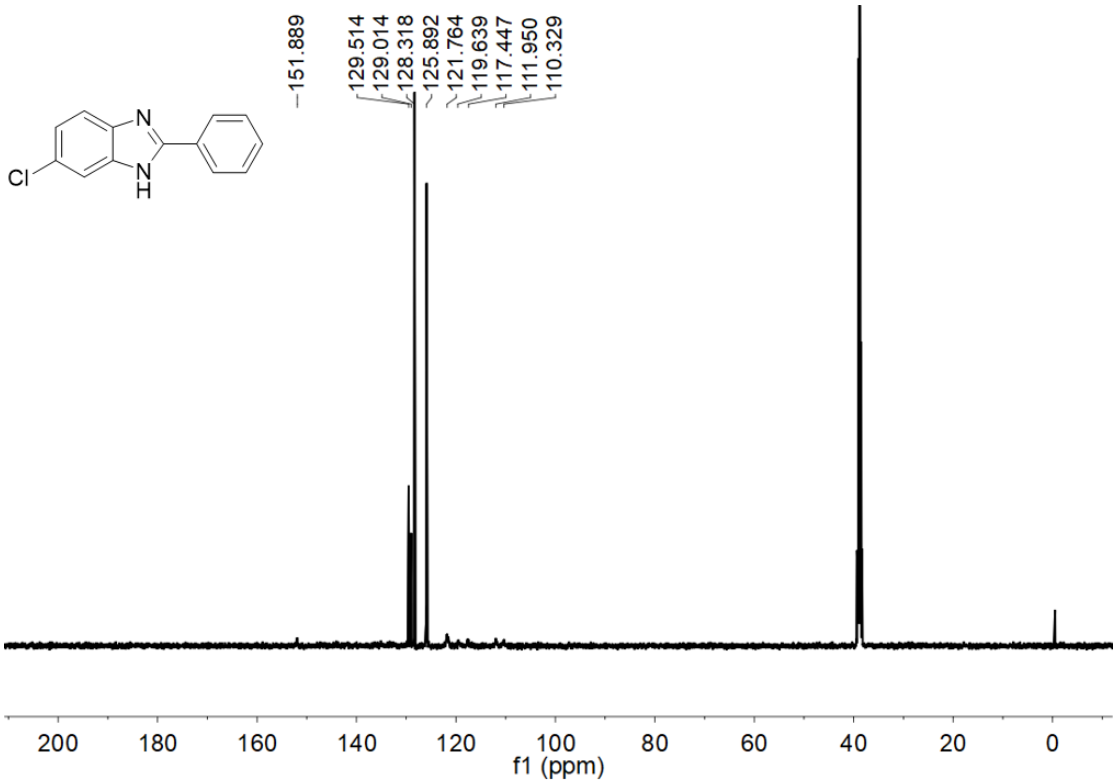

Fig. S57 ^{13}C NMR of 3v in DMSO.

^{1}H and ^{13}C Spectra of compound 3w (DMSO)

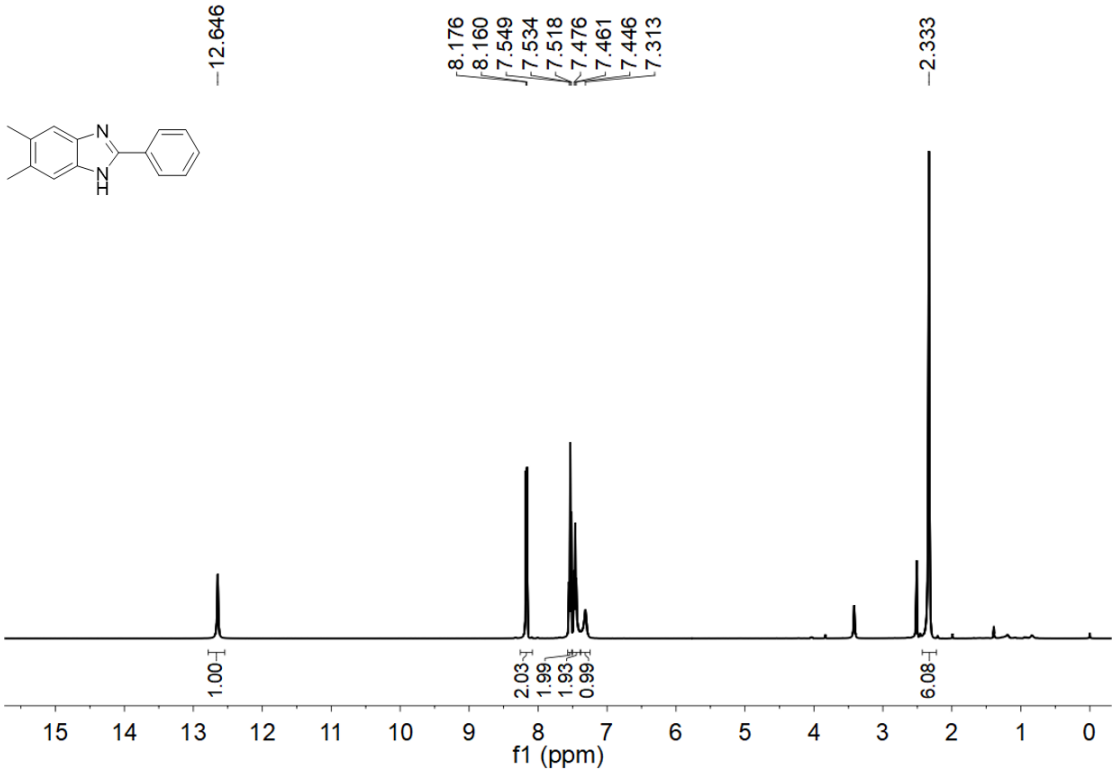

Fig. S58 ^{1}H NMR of 3w in DMSO.

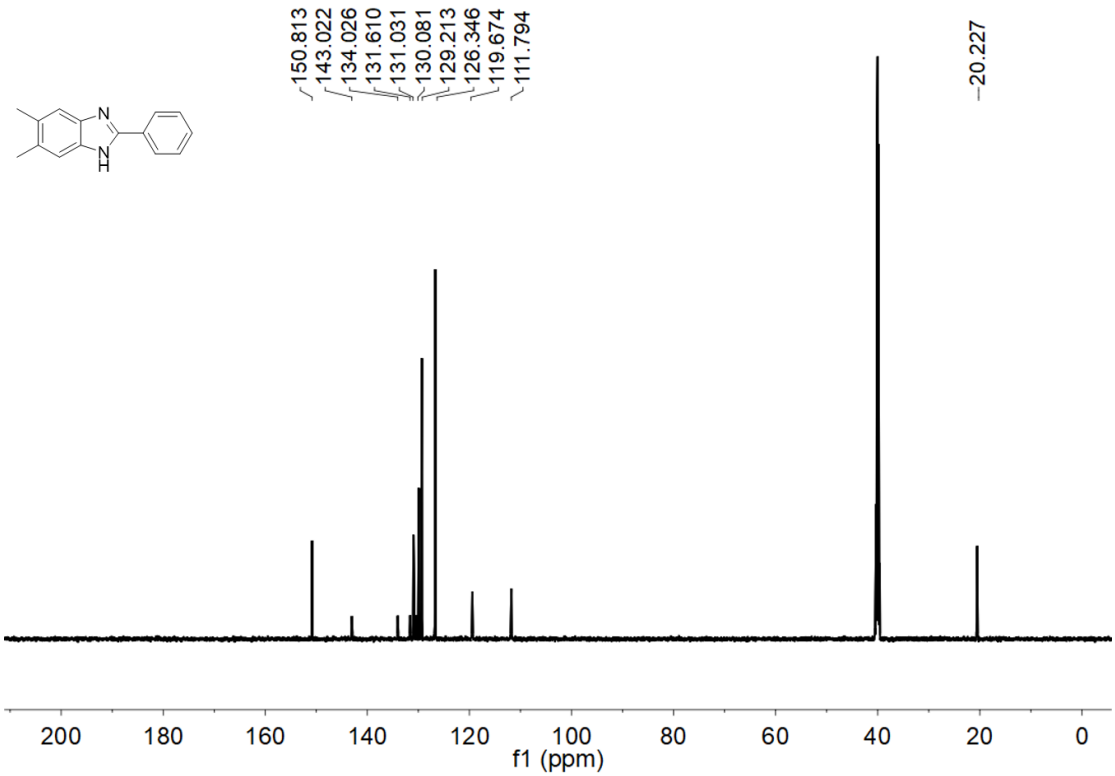

Fig. S59 ^{13}C NMR of 3w in DMSO.

References

[1] H. Bohra, M. Wang, ACS Appl. Polym. Mater. 1 (2019) 1697–1706.

[2] Y. Xu, L. Chen, Z. Guo, et al., J. Am. Chem. Soc. 133 (2011) 17622−17625.

[3] M. J. Frisch, G. W. Trucks, H. B. Schlegel, G. E. Scuseria, M. A. Robb, J. R. Cheeseman, G. Scalmani, V. Barone, G. A. Petersson, H. Nakatsuji, X. Li, M. Caricato, A. V. Marenich, J. Bloino, B. G. Janesko, R. Gomperts, B. Mennucci, H. P. Hratchian, J. V. Ortiz, A. F. Izmaylov, J. L. Sonnenberg, D. Williams-Young, F. Ding, F. Lipparini, F. Egidi, J. Goings, B. Peng, A. Petrone, T. Henderson, D. Ranasinghe, V. G. Zakrzewski, J. Gao, N. Rega, G. Zheng, W. Liang, M. Hada, M. Ehara, K. Toyota, R. Fukuda, J. Hasegawa, M. Ishida, T. Nakajima, Y. Honda, O. Kitao, H. Nakai, T. Vreven, K. Throssell, J. A. Montgomery, Jr., J. E. Peralta, F. Ogliaro, M. J. Bearpark, J. J. Heyd, E. N. Brothers, K. N. Kudin, V. N. Staroverov, T. A. Keith, R. Kobayashi, J. Normand, K. Raghavachari, A. P. Rendell, J. C. Burant, S. S. Iyengar, J. Tomasi, M. Cossi, J. M. Millam, M. Klene, C. Adamo, R. Cammi, J. W. Ochterski, R. L. Martin, K. Morokuma, O. Farkas, J. B. Foresman, D. J. Fox, Gaussian 16, Revision C.01, Gaussian, Inc., Wallingford CT, 2016.